Journal of Ecological Engineering, 2026, 27(1), 301–324 https://doi.org/10.12911/22998993/209959 ISSN 2299–8993, License CC-BY 4.0

Published: 2025.11.25

Received: 2025.08.11 Accepted: 2025.09.27

Formation of the complex of soil aggregate-structural parameters under the influence of green manure application of oilseed radish

Yaroslav Tsytsiura¹

¹ Vinnytsia National Agrarian University, Sonyachna St. 3, 21008 Vinnytsia, Ukraine E-mail: yaroslavtsytsyura@ukr.net

ABSTRACT

Over 12 years, a comprehensive assessment was conducted on the effectiveness of systematic intermediate green manuring using oilseed radish, considering its impact both on the fractional composition of soil and on the main indicators of its structural-aggregate composition, with an evaluation of the potential formation of soil degradation resistance through the assessment of several identification parameters for the 0-30 cm soil layer. A wide range of methods and integrated criteria recommended by global practice for studying the agrophysical properties of soils were used to obtain the data. It was established that oilseed radish, producing a total green manure biomass of 24.01 t ha⁻¹ (4.02 t ha⁻¹ in dry matter), provides a level of bio-organic fertilization equivalent to 14.41 t ha⁻¹ of cattle manure. The application of this green manure allowed optimization of the complex of aggregate-structural soil parameters according to the following criteria: an integrated increase of 6.51% in the complex of agronomically valuable soil aggregate fractions (water-regulating, anti-deflationary, water-stable); stabilization and optimization of soil structure according to the soil stability index (SSI), stable aggregates index (SAI), stable macroaggregates index (SMaI), and coefficient of structurality (Cs), with a resultant growth index of 1.44 compared to the control variant without green manure. A general reduction was achieved in the variability component of the ranking of morphometric parameters of soil aggregates, their fractal dimension, the length criterion of soil structural aggregates (D), and the proportion of aggregate destruction (PAD), with reduction indices of 1.13, 1.04, 1.70, and 1.13, respectively. Under these conditions, the effective impact of green manuring was found to be optimally combined with the observed increase in soil phytotoxicity, with an acceptable frequency of systematic oilseed radish green manure application on the same field not exceeding once every two years.

Keywords: dry soil sieving, wet soil sieving, soil aggregate fractions, soil aggregate water stability, dimensional indices of soil structural-aggregate state.

INTRODUCTION

Green manure technologies are considered an effective and highly promising alternative to conventional fertilization methods for agricultural crops, fully mimicking natural processes of organic matter cycling and the essential macroand micronutrients within the closed loops of agrobiogeocenoses (Toungos and Bulus, 2019; Kaletnik and Lutkovska, 2020; Lutkovska and Kaletnik, 2020). This aligns positively with the global trend toward organic soil management systems according to the strategy outlined in the European Green Deal (Tokarchuk et al., 2024). The

benefits of green manuring are based on shifts in the dynamics of mineralization and humification processes toward dominant humification, which ultimately leads to intensified accumulation of organic carbon, enhanced soil aggregation and structuring, and the formation of conditions that improve the technological quality of the soil profile in terms of its cultivation systems (Lei et al., 2022; Lee et al., 2023; Butenko et al., 2025). This ensures sustainable optimization of the soil's structural-aggregate and agro-physical-technological status, reducing the energy intensity of tillage systems while increasing overall soil workability (Bulgakov et al., 2023).

Positive effects of green manuring have been noted regarding reduced soil bulk density (Abdulraheem and Tobe, 2021), increased porosity, and growth in the proportion of agronomically valuable soil structure fractions, especially those with water-stable characteristics (Lee et al., 2023). Green manuring is also recognized as a key element in optimizing the physical properties of soil, loosening the plow layer, structuring the soil, and increasing its resistance to compaction damage (Talgre, 2013; Hansen et al., 2022). At the same time, it is noted that the positive aftereffect of green manures is determined both by the species-specific characteristics of the green manure crop, the hydrothermal and soil conditions of the respective territories, and by the very technology of green manuring itself (Ma et al., 2021). The duration of this effect generally averages 2-4 years and depends on the level of agricultural land-use intensity and the type of crop rotation according to the species composition of agricultural crops (Jia et al., 2024).

It is noted that the successful choice of specific green manure plant species is fundamental for realizing the positive potential of this technology. The relevance of this approach is confirmed by the existence of over 60 green manure plant species (Green Manure Global Market Report, 2024), which creates practical challenges both in selecting the optimal species for green manuring and in adapting green manure technologies. Moreover, recent global climate and agrotechnological changes have prompted a reassessment of the appropriateness of certain green manure species that until recently were considered mainstays in specific regions (Liu et al., 2020; Abdelrahman et al., 2022).

The above arguments demonstrate the relevance of research on the effectiveness of green manure species adapted to soils with medium fertility potential under conditions of unstable moisture supply, which corresponds to the dominant soil cover and hydrothermal regimes of vegetation across most agricultural territories (Kopittke et al., 2019).

The positive effect of crop rotation, designed on the basis of alternating different biological groups of plants, on the optimization of the soil's structural-aggregate state and physical properties has been generalized and confirmed. According to the results of a meta-analysis of 2.199 paired observations from 53 studies, crop rotation improved the proportion of macroaggregates (>0.25 mm) by 7-14% and aggregate stability by 7-9%. The variance partitioning analysis revealed that variations in crop rotation-induced changes in soil aggregation and associated with organic carbon content were mainly explained by climate (26–35%) and soil properties (17–34%). (Zheng et al., 2023). For these reasons, it is important to assess the effectiveness of the studied agrotechnological solutions specifically within the system of crop rotations adopted in a given region, which makes it possible to effectively adapt their subsequent use and practical implementation. (Meng et al., 2025). In this context, oilseed radish (Raphanus sativus L. var. oleiformis Pers.) is considered an effective candidate for green manure bioorganic technologies. Accompanying studies have demonstrated its high overall bioproductive and adaptive potential for areas with sufficient and unstable moisture on soils with low fertility potential (Tsytsiura, 2020; Tsytsiura, 2025). Against the background of its established value in terms of the biochemical composition of the leaf-stem biomass, as an additional factor in bio-organic fertilization systems, this allowed the species, within a multi-criteria analysis framework, to be classified as a potentially highly effective green manure crop (Tsytsiura, 2024 a,b). However, despite the outlined potential, research results on the impact of its long-term and systematic application as green manure in crop rotation on the structural-aggregate state of the soil and the complex of its agrophysical properties are practically absent. This determined the choice of oilseed radish as the object of longterm studies in the specified evaluation direction, the results of which are presented in this article.

MATERIALS AND METHODS

The research was conducted from 2014 to 2025 at the experimental field of Vinnytsia National Agrarian University (coordinates: 49°11′31″ N, 28°22′16″ E) on grey forest soils – classified as Greyi-Luvic Phaeozems (Phaeozems Albic, Dark Gray Podzolic Soils) under WRB and Haplic Greyzems under FAO with silt loam texture. Baseline fertility indicators of the 0–30 cm soil layer at trial initiation were: humus content 2.68%; available hydrolyzable nitrogen 81.5 mg kg₋₁; extractable phosphorus 176.1 mg kg⁻¹; exchangeable potassium 110.8 mg kg⁻¹; and pH_(KCI) 5.8.

The experimental design involved comparing two successive treatments: a control without green manure and a green manure treatment using oilseed radish on the same plots, rotated every two years to prevent potential phytotoxicity associated with repeated use of cruciferous green manure crops (according to Grodzinsky, 1973; Duff et al., 2020). Both treatments were incorporated into a crop rotation system without the inclusion of other cruciferous plants. During the period 2014-2024, the experiment was conducted following this crop rotation sequence: grain sorghum (2014) - pea (2016) - soybean (2018) - sunflower (2020) chickpea (2022) - grain maize (2024). The overall crop rotation scheme for 2014-2024 was: grain sorghum - spring barley - pea - spring barley soybean - spring wheat - sunflower - winter pea - chickpea - spring barley - grain maize. Soil sampling plots were spatially fixed and were not fertilized with mineral fertilizers throughout the entire experimental period. Measurements were taken at the start in 2014, mid-term in 2019, and final in 2025 (spring, before sowing the respective crop). The experimental plots were arranged in quadruplicate, with a plot size of 25 m². The oilseed radish variety 'Zhuravka' was used in the research. A green manure cropping system was applied, with a seeding rate of 2.5 million seeds per hectare and a row spacing of 15 cm. Sowing was carried out immediately after harvesting the preceding crop, following intermediate combined tillage (flat cutter plus rotary loosening with leveling) to a depth of 12-16 cm. Green manure incorporation was performed when the oilseed radish reached the flowering stage (BBCH 64-67, the optimum phase for green manure), which typically occurred in the second or third decade of October. The green manure was incorporated into the soil to a depth of 14-16 cm every year using heavy disc harrows, following mowing and shredding. The tillage depth during the non-green manure period depended on the crop in the rotation, with an average depth of 22.55 ± 6.31 (SD) cm.

The growth stage of plants was identified відповідно BBCH scale for red oils (Test Guidelines, 2017).

The aboveground mass of plants was carried out by the method of trial plots (1 m^2) (4 in each replication and weighing (WALCOM LB3002 (\pm 0.01 g)). Root biomass was determined using the Profile Wall and Monolith Method (detailed in Tsytsiura, 2025). The dry matter (DM) content in both the aboveground and root plant biomass

was measured by drying to a constant weight at 105 °C and ashing at 550 °C.

The conversion of the total green manure biomass of oilseed radish into classical semi-composted cattle manure was carried out based on a prolonged accompanying biochemical assessment of oilseed radish (Tsytsiura, 2024b; Tsytsiura, 2025) and according to statistics provided by Brown (2021).

Soil sampling

Samples were taken from depths up to 30 cm at 10 cm intervals. Disturbed soil samples (approximately 1 kg) were collected from each interval.

Analysis of soil structural-aggregate composition

Particle-size distribution analysis (PSDA) microaggregate composition analysis (MACA) were applied in the study based on dry and wet sieving methods. The dry sieving method was conducted in accordance with the national standard of Ukraine (DSTU ISO 11277:2005, 2005). For each air-dried soil sample (100 g), sieving was performed using mesh sizes of 10 mm, 7 mm, 5 mm, 3 mm, 2 mm, 1 mm, 0.5 mm, and 0.25 mm. The sieve set included a tray to collect the fraction < 0.25 mm, and the top was covered. After shaking for 2 minutes (280-300 shakes per minute), the soil was separated into the following fractions: > 10 mm; 10–7 mm; 7–5 mm; 5–3 mm; 3–2 mm; 2–1 mm; 1–0.5 mm; 0.5–0.25 mm; < 0.25 mm. The percentage of mechanically stable aggregate size classes was determined by weighing. Fractions in the size ranges 0.25-0.05 mm; 0.05-0.01 mm; 0.01-0.005 mm; 0.005-0.001 mm; and < 0.001 mm were measured using a pipette method modified by Kachinsky (DSTU 4730:2007) combined with the aerometric method of Casagrande, as modified by Prószyński (PN-R-4033) (Bieganowski and Ryżak, 2011), based on average values obtained from these methods.

The wet sieving method was also conducted according to the national standard of Ukraine (DSTU ISO 11277:2005, 2005). The procedure used the same mesh sizes as the dry sieving method but included an additional soil sample preparation system for sieving, following the recommendations of Márquez et al. (2004). This preparation involved air drying followed by rapid immersion in water (slaking), and air drying plus

capillary rewetting to field capacity plus 5% moisture (capillary-wetted). Both subsamples were stored overnight in a refrigerator at 4 °C prior to wet sieving. After wet sieving, all fractions were oven-dried at 70 °C, except the large and small macroaggregates obtained after the capillarywetted pretreatment. These macroaggregates were air dried and later used for the separation of large and small stable macroaggregates. Mass of stable coarse particles or sand retained (inert, not counted as aggregates) was determined by drying followed by treatment with a dispersing agent (5% sodium pyrophosphate) under intensive mechanical stirring. After dispersion, the material was sieved again through the same sieve, and the residue on the sieve was classified as stable coarse particles (sand). The obtained data were used to calculate water stable aggregates (WSA) according to Equation 1, following ISO 10930:2012 (2012):

$$WSA = \left[\frac{(W_a - W_c)}{W_O}\right] \times 100 \tag{1}$$

where: W_a – weight of material on the sieve after wet sieving; W_c – weight of coarse material in size; W_o – weight of aggregates placed on the sieve prior to wet sieving.

Based on the combination of PSDA and MACA analytical methods, the following were additionally determined:

• Dispersion factor (Fd, %) (Equation 2):

$$Fd = \frac{< 0.001 \, mm_{dispers} \, (MACA)}{< 0.001 \, mm \, (PSDA)} \times 100(2)$$

where: < 0.001 mm_{dispers} (MACA) – content of the non-coagulated fraction < 0.001 mm for microaggregate composition analysis (MACA); < 0.001 mm is the sum of the specified fractions for particle-size distribution analysis (PSDA).

• The degree of incorporation (DI) of elementary soil particles into microaggregates (Equation 3):

$$DI = \frac{(< 0.001 \ mm \ (PSDA) \ -}{-< 0.001 \ mm_{dispers} \ (MACA)} \times 100^{(3)}$$

$$(< 0.001 \ mm \ (PSDA))$$

All values are the same as those for Equation 2.

• Fageler's structure factor (FSF) was calculated using Equation 4:

$$FSF = \frac{C_{0.25-1.00 \, mm} + C_{0.05-0.25 \, mm}}{C_{<0.01 \, mm}} \tag{4}$$

where: $C_{0.25-1.00~{\rm mm}(0.05-0.25~{\rm mm/<0.01~mm})}$ – values of individual fraction sizes according to PSDA analysis.

• The mean weight diameter of soil aggregates (for dry (MWD) and wet (MWD_{wet}) sieving), geometric mean diameter of soil aggregates (for dry (GMD) and wet (GMD_{wet}) sieving), and mean weight aggregate stability (MWAS) were calculated following the recommendations of Aksakal et al. (2020) and Zhou et al. (2020) (Equations 5–7).

$$MWD = \sum_{i=1}^{n} (x_i m_i) \tag{5}$$

where: n – the number of aggregate size classes; x_i – mean size class i; and m_i – the weight ratio of soil aggregate (or water-stable aggregate for MWD_{wel}) at the class i.

$$GMD = e^{\sum_{i=1}^{n} \left(\frac{m_i}{m}\right) ln(x_i)}$$
 (6)

where: n – the number of aggregate size classes; x_i – mean size class i; and m_i – soil aggregate (or water-stable aggregate for GMDwet) weight ratio at the class i; m – the total soil mass used in the test.

$$MWAS = \sum_{i=1}^{n} (w_i A S_i) \tag{7}$$

where: n is the number of aggregate size classes; w_i proportional coefficient of each aggregate size class i; AS_i — water aggregate stability of each aggregate size class (%).

• Soil stability index (SSI) was calculated according to Franzluebbers et al. (2022) (Equation 8):

$$SSI = \frac{MWD_{wet}}{MWD}$$
 (8)

where: *MWD* – mean weight diameter of soil aggregates; *MWD*_{wet} mean weight diameter of water-stable soil aggregates.

 Potential structural deformation index (PSDI) (method of Mbagwu and Bazzoffi (1989) (Equation 9)):

$$PSDI = \left[1 - \frac{MWD_{wet}}{MWD}\right] \times 100 \tag{9}$$

The components of the formula are similar to those of Equation 8.

Proportion of aggregate destruction (PAD (%))
were calculated using the aggregate data for
each particle size fraction (calculated according
to Kemper and Rosenau (1986) (Equation 10):

$$PAD = \frac{DR_{0.25-10} - WR_{0.25-10}}{DR_{0.25-10}} \times 100 (10)$$

where: $DR_{0.25-10}$ is the aggregate content (%) with an aggregate size of 0.25–10.0 mm under dry sieving; $WR_{0.25-10}$ is the aggregate content (%) with an aggregate size of 0.25–10.0 mm under wet sieving.

 Stable aggregates index (SAI) (Márquez et al. (2004)) (Equation 11):

$$SAI = \frac{\sum_{j=1}^{n} [(n+1) - j] \times S_j}{\sum_{j=1}^{n} [(n+1) - j] \times T_j} \times 100 \quad (11)$$

where: S_j – the amount of stable aggregates in fraction j. T_j – total amount of aggregates in fraction j (from the capillary-wetted treatment) and n is the total number of size fractions. For j=1 for the largest size class.

• Stable macroaggregates index (SMaI) (Márquez et al. (2004)) (Equation 12):

$$SMaI = \frac{n \sum_{j=1}^{m} [(m+1) - j] \times S_j}{m \sum_{j=1}^{n} [(n+1) - j] \times T_j} \times 100 (12)$$

where: S_j , T_j , n, j – the same in Equation 11; m – the total number of size classes > 0.25 mm.

 Susceptibility of soil to wetting (S_w, %) (Klíč, 2024) (Equation 13):

$$S_w = \frac{MWD - MWD_{wet}}{MWD} \times 100$$
 (13)

• Fractal dimension (FD) of the structural-aggregate state of soil (Equation 14):

$$FD = 3 - \left[\lg \left(\frac{M(r < X_i)}{M_{total}} \right) / \lg \left(\frac{X_I}{X_{max}} \right) \right] (14)$$

where: X_i – the average soil aggregate diameter of any grade, which is numerically equal to the average value of two adjacent sieve holes, for > 5 mm aggregates, the upper limit of aggregate diameter is 10 mm; X_{max} – the average particle size of the maximum particle size, mm; M (r < X_i) – the weight of the aggregate with particle size less than X_i ; and M – the total weight of the aggregates.

 Erodibility (K-factor) (according to Tian et al., 2022) (Equation 15):

$$\times \left\{ \begin{bmatrix} K - factor = 7.954 \times \\ 0.0017 + 0.0494 \times exp \\ \left[-0.5 \times \left(\frac{1.675 + \log_{10} GMD}{0.6986} \right)^{2} \right] \right\}^{(15)}$$

where: *GMD* – geometric mean diameter (GMD, mm) of soil aggregates.

Agrotechnological soil parameters

The coefficient of structurality (Cs) was determined using Equation 16:

$$C_s = \frac{N_v}{N_t} \tag{16}$$

where: N_v – total soil macroaggregates 0.25–10 mm, %; N_t – total fractions < 0.25 mm and > 10 mm, %.

The degree of soil pulverization during tillage upon reaching the soil's physical maturity was determined according to the average separation length criterion of soil structural aggregates (D, mm) after uniform tillage (spring disking with disk harrows to a depth of 10–12 cm). The state of physical maturity of the soil was identified according to the method of Pons and Zonneveld (1965).

The separation length criterion of soil structural aggregates (D) was determined based on the automatic measurement of parameters such as the two Feret diameters (Figure 1) from soil surface photographs using the adapted BASEGRAIN software package (v.2.2.0.4) (detailed methodology in Tsytsiura (2023)) and applying Equation 17 according to Church et al. (1987).

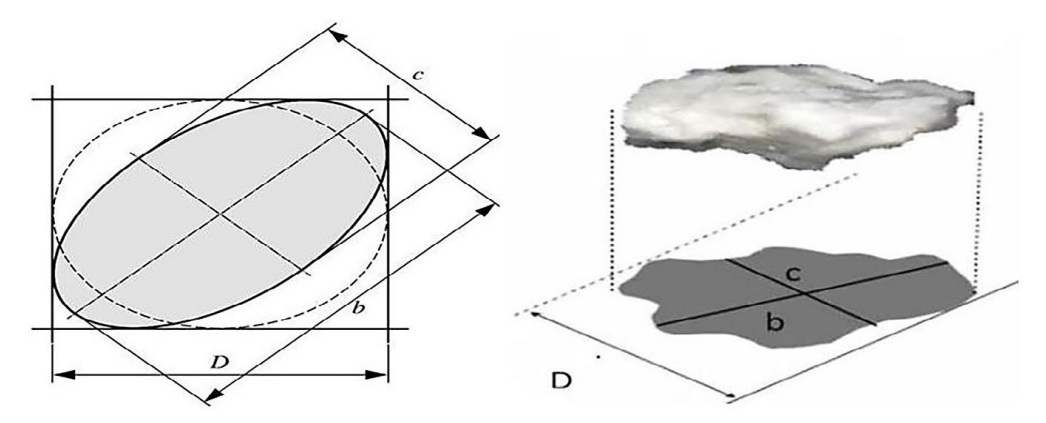


Figure 1. Definition sketch for lengths D, b, and c (according to Stähly et al. (2017))

$$D = b \times \left(\frac{1}{\sqrt{2}} \times \left[1 + \left(\frac{c}{b}\right)^2\right]^{0.5}\right) \tag{17}$$

where: b – vertical and c – horizontal Feret diameter, mm; D – separation length criterion, mm.

The images were captured using a Canon EOS 750D Kit 18-135 mm IS STM DSLR camera with an additional Canon EF 100 mm f/2.8 Macro lens with a UV filter in an orthogonal projection to the soil surface using a standard scale ruler under artificial shading according to Xingming et al. (2021).

To assess the level of soil phytotoxicity under the systematic use of oilseed radish, a biotesting method was applied (at the same key accounting dates - 2019 and 2025) using the standardized approach widely recognized in allelopathic practice as the method of conditional coumarin units (CCU) (Grodzinsky, 1973; Tsytsiura and Narwal, 2025). One conditional coumarin unit corresponds to a reference solution of the natural growth inhibitor coumarin (2H-chromen-2-one or 2H-1-benzopyran-2-one) – a lactone of o-hydroxycinnamic acid – at a concentration of 1 g 1-1. Garden cress (Lepidium sativum L.) was selected as the biological test object. The recalculation of germination and the pattern of morphological development of garden cress plants on soil substrates (aken from the 0-10, 10-20, and 20-30 cm soil layers) with different durations of oilseed radish green manuring into conditional coumarin units was carried out based on regression equations constructed according to the scale presented in Grodzinsky (1973). The control variant of the testing was carried out without the use of green manuring.

To analyze the hydrothermal conditions, the following were applied: average daily temperature (°C), precipitation (mm), hydrothermal coefficient (HTC) (Equation 18), and the coefficient of significance of deviations (Csd) (Equation 19) (Table 1).

$$HTC = \frac{\sum R}{0.1 \times \sum t_{>10}}$$
 (18)

where: ΣR – the sum of precipitation (mm) over a period with temperatures above 10 °C, $\Sigma t_{>10}$ – the sum of effective temperatures over the same period. Ranking of HTC values conditions: HTC > 1.6 - excessivehumidity, HTC 1.3-1.6 - humid, HTC 1.0–1.3 – moderately dry, HTC 0.7–1.0 – dry, HTC 0.4–0.7 – very dry.

$$C_{sd} = \frac{\left(X_i - X_{av}\right)}{S} \tag{19}$$

where: Xi – current weather element;

 X_{av} – average long-term value; S – standard deviation; i – ordinal number of the year.

 C_{sd} level: $0 \div 0.5$ (-0.5) – conditions close to normal; (-1) 1 ÷ (-2) 2 – significantly different from long-term values;

2 (< -2) – close to extreme conditions.

Statistical processing

The indicators of variation statistics were determined using the generally accepted calculation method as outlined in Stoyan & Unland (2022) and Wong (2018) in the statistical software Statistica 10 (StatSoft - Dell Software Company, USA). For each analyzed physical

Golger enmance enablinearion), 2011–2021 (compared to the long term average period of 2002–2013)															
	Precipitation amount, mm	*t _{aver} , °C (IV-X)			I	_		**							
Year			V		VI		VII		VIII		IX		C _{sd aver} V–IX	*t aver, °C	Precipitation
	(IV-X)	(*****)	X _i	C _{sd}			amount, mm								
2014	590.4	14.62	3.93	3.39	1.55	1.00	1.31	0.24	1.05	0.46	1.25	1.10	1.24	0.2	245.5
2015	303.1	15.48	0.92	0.19	0.72	-0.53	0.32	-1.16	0.12	-1.13	1,184	0.97	-0.33	9.5	256.1
2016	406.1	15.33	0.49	-0.26	1.27	0.48	1.06	0.39	0.90	0.46	0.01	-1.17	-0.02	-0.6	325.7
2017	443.1	15.04	0.78	0.04	0.50	-0.92	1.52	1.38	0.82	0.30	3.10	4.47	1.05	-0.4	323.7
2018	444.2	16.39	0.31	-0.45	4.40	6.28	2.16	2.71	0.59	-0.19	1.38	1.33	1.94	0.0	271.0
2019	560.2	15.70	4.90	4.42	1.68	1.25	1.01	0.30	0.24	-0.90	0.99	0.62	1.14	2.9	200.5
2020	589.2	15.64	5.33	4.87	1.55	1.01	0.59	-0.59	0.53	-0.30	0.86	0.38	1.07	-0.3	356.1
2021	459.7	14.33	3.13	2.54	1.68	1.25	0.78	-0.19	1.46	1.61	0.71	0.10	1.06	1.2	216.9
2022	678.7	15.15	1.43	0.74	1.50	0.91	0.90	0.06	1.71	2.13	4.96	7.86	2.34	2.2	278.0
2023	486.9	16.24	0.09	-0.69	1.64	1.18	1.41	1.14	0.65	-0.05	1.02	0.66	0.45	2.9	371.2
2024	481.9	17.94	0.58	-0.17	1.66	1.21	1.19	0.67	0.77	1.46	0.45	-0.38	0.41	1.2	263.8

Table 1. Assessment of hydrothermal regimes (by the indicator of HTC) (Dfa/Dfb zone according to the Köppen–Geiger climate classification), 2014–2024 (compared to the long-term average period of 2000–2013)

Note: *average daily temperature (°C) for the period from November of the previous year to March of the following year; **total precipitation (mm) for the period from November of the previous year to March of the following year.

parameter of soil determined its arithmetic mean, standard deviation (SD) and coefficient of variation (C_v). Analysis of variance was used to compare the differences between means among treatments by the Bonferoni test at a statistical level of p < 0.05 and p < 0.01. The data obtained were analyzed using the analysis of ANOVA.

RESULTS AND DISCUSSION

During the period of intermediate green manure use of oil radish, according to the experimental scheme, its average green manure productivity was 24.01 t ha⁻¹ (4.02 t ha⁻¹ in dry matter) with interannual variation (for Cv) of 31.55% (28.53%) (Figure 2). The average ratio coefficient between the formed aboveground biomass and root residues was 3.52 in fresh biomass and 2.34 in dry matter.

Considering the obtained level of green manure bioproductivity, the interannual variation of the indicator under conditions of pronounced unstable moisture (Dfa/Dfb) (Table 1), and the long-term system for assessing potential cruciferous plant species (Duff et al., 2020), oil radish was classified as an adaptive species suitable for intermediate summer green manuring in the bio-organic fertilization system for non-cruciferous crops. This aligns positively with the minimum threshold level of bioproductivity at up to 2 t ha⁻¹ in dry matter as

a criterion for effective green manure potential (Talgre, 2013; Singh et al., 2023).

This is also confirmed by the determined fertilizing potential of oil radish as a green manure, expressed in terms of semi-decomposed cattle manure equivalent, amounting to 16.85 t ha⁻¹ for the period 2014-2019 and 11.96 t ha⁻¹ for the period 2020-2024, which corresponds to the above-average category. A positive effect of systematic green manuring of varying application durations on changes in the soil's structuralaggregate composition and the ratio of several important fractions was identified (Table 2). It was established that, compared to the control, the green manuring variant, on average for the 0-30 cm soil layer at the first comparison date (2019), reduced the absolute value of the cloddy fraction (>10 mm) by 4.92% and the dust fraction (<0.25 mm) by 1.41%, while increasing the agronomically valuable fraction (10-0.25 mm) by 6.32%. At the final accounting date (2025), an accumulated positive effect of green manuring on the formation of similar indicators was observed, amounting to 7.70%, 1.34%, and 9.04%, respectively.

At the same time, for the control variant under this crop rotation system and complete absence of fertilization, a gradual degradation of the soil was recorded in terms of the optimality parameters of its structural-aggregate composition.

The results of phased comparisons conducted in 2019 and 2025 confirm these findings. In

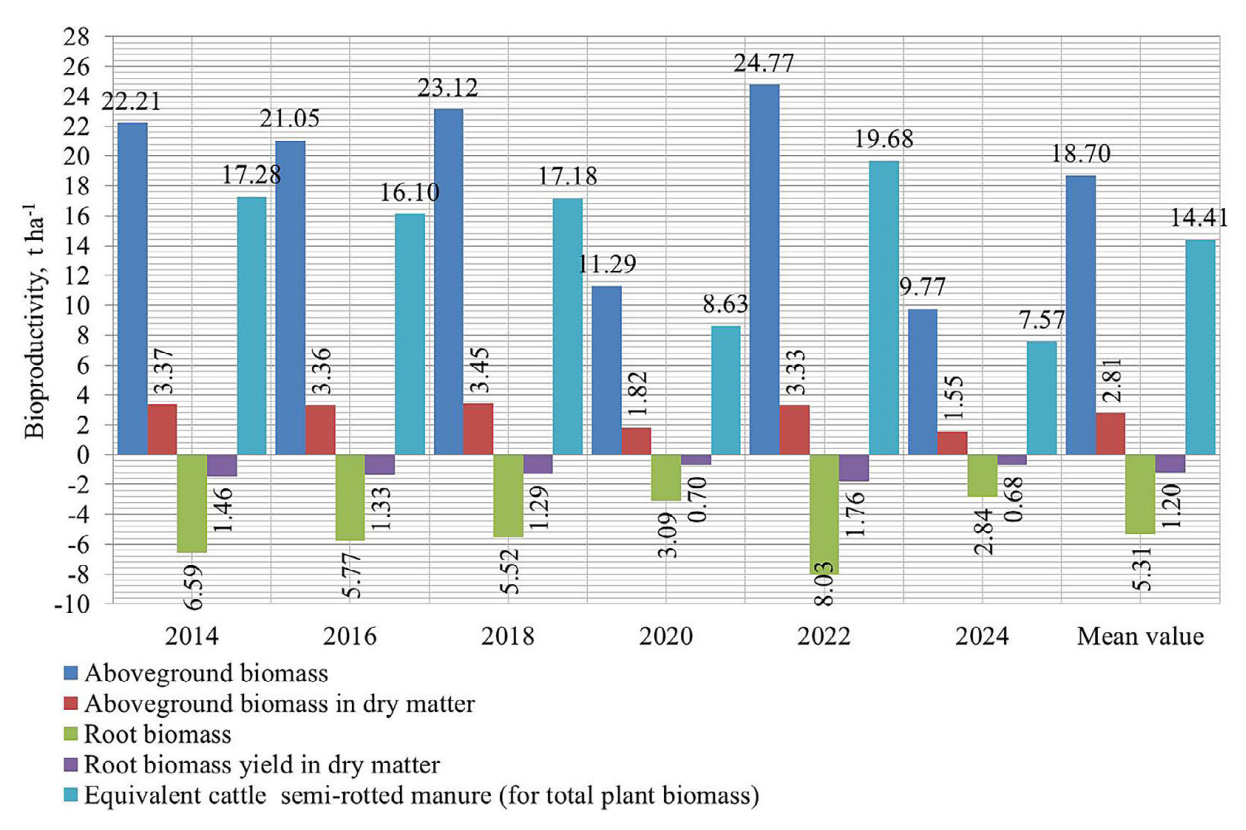


Figure 2. Indicators of green manure bioproductivity of oilseed radish for the summer intermediate sowing date (at the flowering stage, BBCH 64–67), t ha⁻¹ (LSD_{0.5} 1.07 – for aboveground biomass; 0.29 – for aboveground biomass in dry matter; 0.58 – for root biomass; 0.17 – for root biomass yield in dry matter; 0.84 – for equivalent cattle semi-rotted manure)

2019, relative to the baseline values of 2014, the average soil layer (0-30 cm) showed an increase in the coarse fraction (>10 mm) by 1.62%, an increase in the dust fraction (<0.25 mm) by 1.70%, and a decrease in the sum of fractions between 10-0.25 mm by 2.99%. By the terminal assessment date in 2025, a similar trend was observed compared to the initial 2014 control variant, with increases of 2.01%, 3.74%, and a decrease of 5.73%, respectively. Over the 12-year period, the control variant demonstrated dynamic processes of intensive differentiation in the structural-aggregate composition, with simultaneous growth of both the coarse (>10 mm) and dust (<0.25 mm) fractions. These changes in the fraction structure ratios during dry sieving indicate active microaggregation processes.

According to several studies (Le Bissonnais, 2016; Medvedev et al., 2020; Nurhartanto et al., 2022; Usman and Jayeoba, 2025), simultaneous increases in both coarse and dust fractions signal granulometric internal degradation of the soil and serve as a precursor to significant deterioration in the associated properties.

In this regard, sustainable green manuring with oilseed radish optimizes the balance of soil fractions. This is further supported by the reduced variability of fractional shares across the entire analysis range: over the full cycle of green manure application, total inter-fraction variability decreased by 16.31% compared to the 2014 baseline, whereas in the variant without green manure it increased by 5.47%. Following Stoyan & Unland (2022), this indicates an increase in the overall dispersion of the soil's structuralaggregate system, leading to adverse changes in related soil regimes. Amid the observed structural shifts, changes in individual fraction shares were also noted. In the green manure variant at the final assessment in 2025, compared to the 'Control II' variant, there was an overall increase in the 10-7 mm fraction by 2.57% and a decrease in the 0.5–0.25 mm fraction by 4.48%. The greatest increase was seen in the 5-3 mm fraction, rising by 10.99%. Compared to the absolute control (2014 baseline), fractions within the 0.5–7 mm range increased on average by 8.74%, with a peak increase of 5.33% in the 3-2 mm fraction.

Table 2. Dynamics of soil structural-aggregate composition depending on the experimental variants
(PSDA analysis, dry sieving, for the comparable period 2014–2025), %

Evporimental	Soil				The	percentage of silt (0.002- 0.05 mm) (<0.002 mm) 63.97a 22.52a 62.37b 23.36a 63.95a 23.09a 63.48a 24.59b 63.54a 24.31b 64.52c 24.99b 61.11d 22.21a 61.41d 22.60a							
Experimental variant	layer, cm	> 10	10–7	7–5	5–3	3–2	2–1	1–0.5	0.5– 0.25	<0.25	sand (0.05– 2.00 mm)	(0.002-	(<0.002
2014													
At the	0–10	25.32a	10.83ª	9.21ª	15.41ª	7.82ª	12.27ª	6.22ª	4.17ª	8.75ª	23.84ª	63.97ª	22.52ª
beginning of experiment	10–20	27.17 ^b	11.04 ^b	8.71 ^b	15.51⁵	7.14 ^b	14.12 ^b	5.15⁵	3.09 ^b	8.07 ^b	23.51ª	62.37 ^b	23.36ª
(absolute control)	20–30	30.25°	10.89ª	8.59 ^b	14.56°	6.55°	12.69°	5.33°	2.88°	8.26 ^b	21.97ª	63.95ª	23.09ª
2019													
Control I	0–10	27.14a	8.91ª	8.51a	11.96ª	5.91a	14.39ª	7.05a	6.01a	10.12a	28.66b	63.48ª	24.59b
(without green manure)*	10–20	29.09b	8.19 ^b	6.72b	12.26b	6.11 ^b	15.29⁵	6.68 ^b	5.91⁵	9.75⁵	29.06b	63.54ª	24.31 ^b
	20–30	31.37°	8.85°	6.06°	12.24 ^b	5.51°	13.53°	7.07ª	6.05ª	10.32ª	27.73b	64.52°	24.99 ^b
Green	0–10	22.28ª	12.46ª	11.32ª	18.88ª	9.84ª	11.21ª	4.07ª	2.72ª	7.22ª	19.20°	61.11 ^d	22.21ª
manure	10–20	22.69ª	12.24ª	10.98⁵	19.05⁵	10.69b	12.08b	3.27b	2.11 ^b	6.89b	18.56°	61.41 ^d	22.60a
application I**	20–30	23.02b	11.53 ^b	10.75⁵	19.28⁵	9.65ª	12.17b	3.43 ^b	3.42℃	6.75⁵	19.97 ^d	63.01 ^b	22.98ª
						202	25						
Control II	0–10	28.18ª	8.94ª	6.54ª	9.47ª	5.43ª	14.89ª	6.74ª	7.59ª	12.22ª	30.46e	63.59ª	26.29°
(without green	10–20	28.85b	9.03ª	6.63a	9.12 ^b	5.72b	14.07b	6.57ª	7.92 ^b	12.09ª	29.85e	64.02ª	25.33b
manure)***	20–30	31.67°	8.88ª	5.57a	10.21°	5.47a	13.21°	5.84ª	7.16°	11.99ª	27.26b	64.65°	26.56°
Green	0–10	19.02a	10.92ª	12.41ª	20.24ª	12.48ª	11.05ª	3.05ª	3.27ª	7.56ª	18.65°	62.59b	20.44 ^d
manure application	10–20	20.19 ^b	11.72 ^b	11.49 ^b	20.87b	13.12 ^b	10.75⁵	2.78ª	2.76 ^b	6.32 ^b	18.38°	62.42 ^b	19.20e
II****	20–30	20.42b	11.92 ^b	11.35⁵	20.66b	11.89°	11.24ª	2.11⁵	3.22a	7.19°	17.78 ^f	63.79ª	19.43e

Note: Crop rotation on the plot: grain sorghum (2014) – spring barley (2015) – pea (2016) – spring barley (2017) – soybean (2018); Use of intermediate green manure in the crop rotation scheme on the plot: grain sorghum (2014) – pea (2016) – soybean (2018); Crop rotation on the plot: spring wheat (2019) – sunflower (2020) – winter pea (2021) – chickpea (2022) – spring barley (2023) – maize for grain (2024); Use of intermediate green manure in the crop rotation scheme on the plot: sunflower (2020) – chickpea (2022) – maize for grain (2024). Different lowercase letters in the table indicate significant differences among treatments within the same soil layer (p < 0.05).

In the 'Control II' variant, compared to the absolute control, the fractions in the 2-<0.25 mm range increased by 9.77%, with the greatest growth (3.74%) occurring in the <0.25 mm fraction. Although similar trends regarding green manure's impact on soil structural-aggregate composition have been observed in other studies (Le Bissonnais, 2016; Lee et al., 2023; Li et al., 2024; Li et al., 2025), some differences should be noted. Specifically, simultaneous decreases in the >10-7 mm and 0.5-<0.25 mm fractions alongside increases in intermediate fractions support the positive role of long-term green manure application in enhancing soil structure by increasing the macroaggregate fraction within the 2.0-5.0 mm range. Based on Gentsch et al. (2024), the applied green manure regime balances the soil aggregate structure while maintaining sufficient dispersion to optimize water absorption and preserve porosity constants.

Conversely, intensive use of gray forest soil without fertilization in the control variant – characterized as a degenerative land use system by Rezáčová et al. (2021) and Peng et al. (2024) – leads to disruption of stable macroaggregate intervals, increased overall dispersion, and deterioration of agro-physical and hydrological constants. Medvedeva et al. (2020) also noted that gray forest soils under intensive agriculture without organic matter replenishment experience progressive structural degradation, especially in the upper horizons.

From this perspective, the application of oilseed radish proved effective. The conclusions are supported by changes in the proportion of agronomically valuable fractions determined according to Medvedev et al. (2020) under different experimental variants (Figure 3). It was established that, in comparison of the 'Green manure application II' and 'Absolute

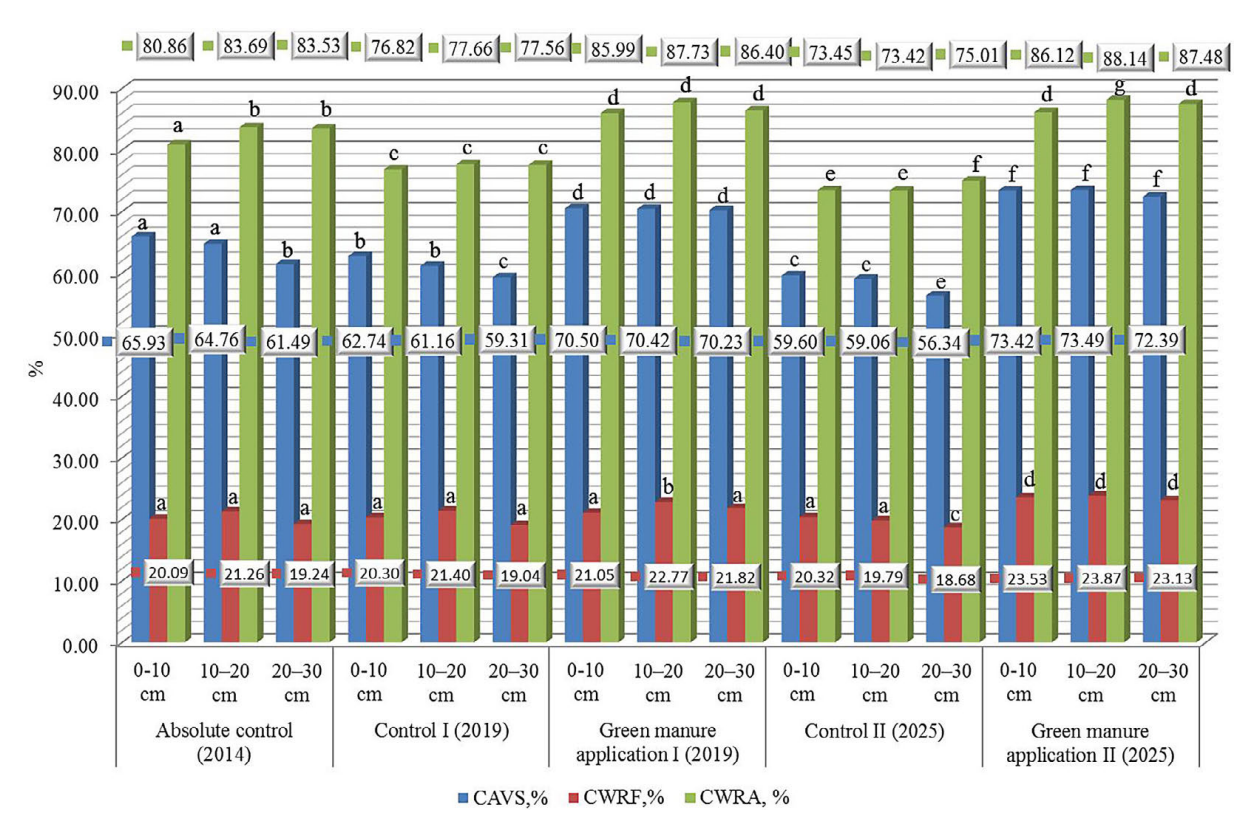


Figure 3. Proportion of agronomically important fractions of the soil structural-aggregate state depending on experimental treatments (for the comparable period 2014–2025), %

Note: CAVS – content of agronomically valuable structure (0.25–10.0 mm, %);

CWRF – content of water-regulating fractions (1.0–3.0 mm, %);

CWRA – content of wind-resistant aggregates (> 1 mm, %).

Explanations of experimental treatments are provided in the footnotes of Table 2.

Different lowercase letters indicate significant differences among treatments at the same soil layer (p < 0.05).

control' variants, the content of the CAVS fraction increased by 9.04%, the CWRF fraction by 3.31%, and the CWRA fraction by 4.56%. Conversely, in the comparison of the 'Control II' and 'Absolute control' variants, these indicators decreased by 5.76%, 0.60%, and 8.73%, respectively. Based on the evaluations by Gentsch et al. (2024), such results demonstrate the antierosion effectiveness of green manure application from both water and wind erosion perspectives, as well as optimization of the soil's water-regulating and water-retaining functions. It should also be noted that soil texture is a relatively stable characteristic, largely dependent on the parent material and soil formation processes, and green manure application has a less significant overall effect on it (Medvedev et al., 2020).

However, in the 'Green manure application II' variant, compared to the absolute control, a decrease in the sand fraction (0.05–2.00 mm) by 4.84% was observed in the 0–30 cm soil layer, along with reductions in the silt (0.002–0.05 mm)

and clay (< 0.002 mm) fractions by 0.50% and 3.28%, respectively. This pattern positively aligns with models of soil aggregation under systematic replenishment of the soil with plant-derived organic matter (Qin et al., 2024), highlighting enhanced involvement of fractions smaller than 0.05 mm and simultaneous intensification of the intra-profile leaching of the finest fractions. This results in certain structural shifts within the main fractions that define soil texture, while the overall soil texture classification remains unchanged.

More significant conclusions regarding the effectiveness of green manure application were drawn based on the analysis of the soil's structural-aggregate composition from wet sieving results (Figure 4).

As a result of the long-term application of oilseed radish as a green manure, compared to the absolute control, an average for the 0–30 cm soil layer showed a consistent decrease in the proportion of fractions in the 1–<0.25 mm range and an increase in the proportion of fractions

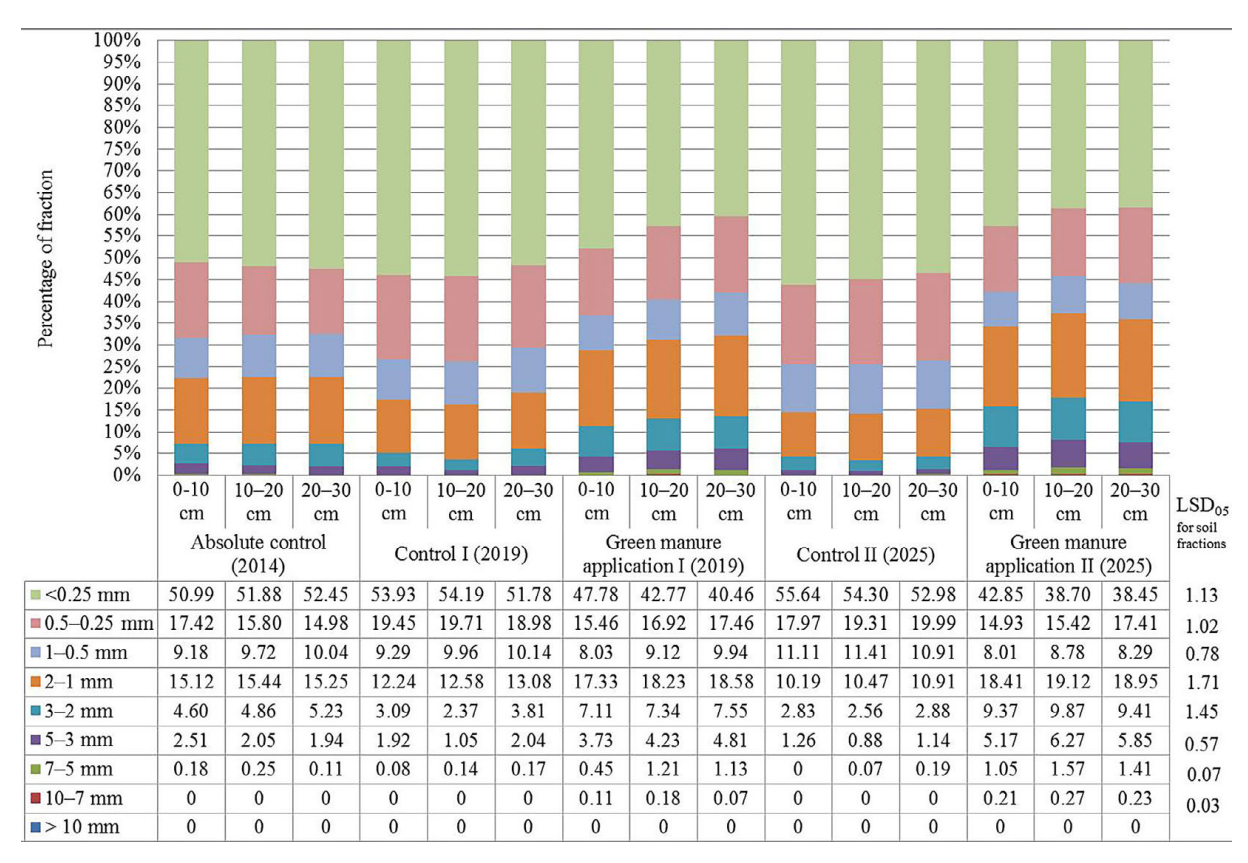


Figure 4. Soil structural-aggregate composition by wet sieving (modified after Márquez et al. (2004)) depending on experimental treatments (for the comparable period 2014–2025), %

in the 2–10 mm range in an equivalent ratio of 13.21%. This process was most pronounced in the 0-20 cm soil layer. Moreover, a growing rate of this dynamic was noted when comparing the measurements from 2019 and 2025, with a growth index of 1.08. In contrast, the 'Control II' treatment, compared to the absolute control, exhibited an opposite trend in fraction formation. These characteristics of fraction formation under wet sieving confirmed the positive effect of green manure biomass through the organic products of its transformation and intensification of the humification process, leading to an increase in the share of water-stable fractions sized 1–3 mm. This increase was 10.72%, 12.79%, and 11.79% for the soil layers 0-10, 10-20, and 20-30 cm, respectively, when comparing the 'Absolute control' and 'Green manure application II' variants. For the 'Control II' variant at the same soil depths on the final observation date, this indicator was significantly lower than in the 'Green manure application II' by 7.95%, 8.44%, and 7.49%, respectively.

These structural changes were noted alongside a simultaneous decrease in the share of fractions

<0.25 mm for the wet sieving variant, with an average reduction of 14.31% in the 0–30 cm soil layer for 'Green manure application II' compared to 'Control II'. Under these conditions, only the green manure treatment variant had water-stable aggregates in the 10–7 mm fraction below 0.50% on both observation dates, and no aggregates were identified in the >10 mm fraction.

Such changes in the structural fraction distribution of water-stable aggregates — with a significant decrease in the upper fractions greater than 7 mm and an intense reduction of fractions smaller than 7 mm, alongside several-fold increases in the 0.5–<0.25 mm fraction interval, characteristic of the experimental soil variants overall — indicate (based on conclusions by Peng et al., 2024) that before the experiment started, soil profile destructuring was already present, which is a clear sign of soil degradation.

The application of green manure contributed to increased water stability of soil aggregates, both due to additional aggregation and increased humification. As a result, this ensured increased hydrophobicity of soil particles, confirmed by several studies (Le Bissonnais, 2016; Tian et al.,

2022; Klíč, 2024). However, the lack of sufficient humification levels in soil aggregates, considering the absence of water-stable macroaggregation for soil fractions in the 7->10 mm range (according to Márquez et al., 2004; Rezáčová et al., 2021; Peng et al., 2024), confirmed that the organic components of green manure using oilseed radish form an effective water-stable structure at the microaggregate level, with the maximal effect observed at a depth of 10-20 cm. This corresponds to the main location of green manure biomass accumulation during its incorporation into the soil. This is confirmed both by research (Li et al., 2024; Li et al., 2025) and visually demonstrated in Figure 5.

In particular, in the variant of sustainable green manure use with oilseed radish at the reporting date (2025), an intensive process of water-stable aggregation formation was observed, with the most pronounced process characteristic for the 10–20 cm soil layer (Figure 5, position II). The

control variant was characterized by the formation of fine microaggregation relatively resistant to water action (Figure 5, positions III-IV). It should be noted that for the control variant in the 0-10 cm soil layer (Figure 5, III), the formation of a so-called dense, continuous, deep-platy structure was identified, mixed with a significant presence of ultrafine microaggregates. This pattern, considering a number of studies (Zhu et al., 2018; Zhou et al., 2020; Yang et al., 2025), indicated a potentially rapid destruction of the observed microaggregates under rainfall, leading to the formation of a deep crusted layer, which aligns with the results of the soil microaggregate analysis (Table 3). Based on the results of the PSDA variant of the microaggregate analysis, changes in the soil microaggregate structure were identified with the application of green manure. These changes, comparing the control variant and the green manure variant at the final assessment date (2025), were characterized by a consistent increase in the

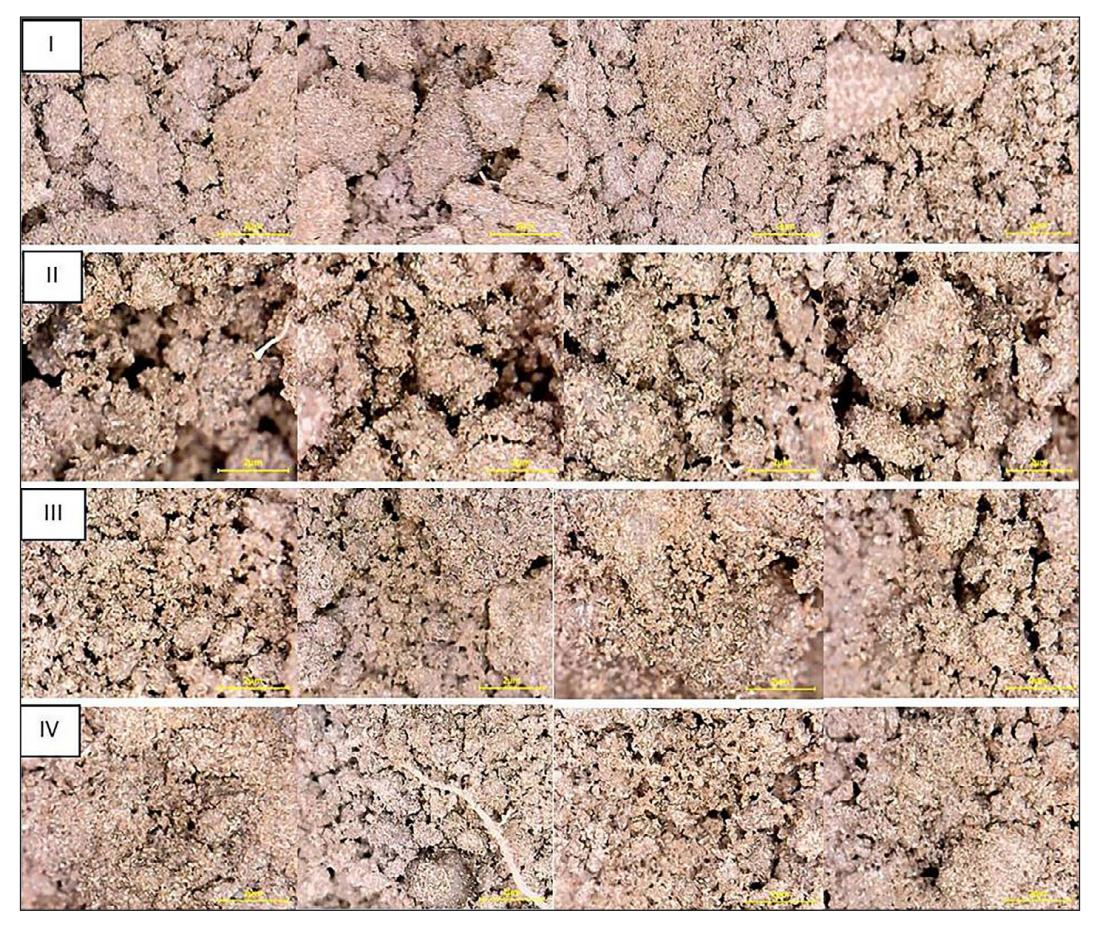


Figure 5. Microphotographs of the surface of soil macroaggregates from different soil horizons depending on the experimental variant (I – for the 0–10 cm soil layer and II – for the 10–20 cm soil layer in the zone of oilseed radish green manure decomposition for the 'Green manure application II' variant III – for the 0–10 cm soil layer and IV – for the 10–20 cm soil layer in the 'Control II' experimental variant), 2025

Table 3. Microaggregate analysis of soil structure depending on experimental variants (for the comparative period 2014–2025 for the soil fraction range 0.25–<0.0001 mm), %

	Soil	Soft Haction	Soil fraction									
Experimental variant	layer, cm	0.25-	0.05-	0.01–0.005	0.005-0.001	<0.001	MWD, mm	GMD, mm	Fd, %	DI, %	FSF	
	0	0.05	0.01		.014							
	0–10	13.51 ± 0.31a	48.27 ± 0.83 ^a	12.77 ± 0.51a	7.33 ± 0.19 ^a	33 ± 0.19 ^a 18.12 ± 0.17 ^a		0.058a	42.05a	57.95ª	0.625°	
	10–20	14.27 ± 0.39 ^b	45.59 ± 1.14 ^b	13.62 ± 0.33 ^b	7.91 ± 0.31 ^a	18.61 ± 0.11 ^a	0.095 ^a	0.058ª	40.30 ^b	59.70b	0.561 ^b	
Absolute	20–30	12.96 ± 0.47°	47.46 ± 0.97 ^a	13.85 ± 0.42 ^b	6.59 ± 0.38 ^b	19.14 ± 0.14 ^b	0.095a	0.057a	38.51°	61.49°	0.535b	
control	0–10	"57.89 ± 1.17ª	25.61 ± 0.49 ^a	12.87 ± 0.17 ^a	2.85 ± 0.11a	0.78 ± 0.09 ^a						
	10–20	57.24 ± 1.29 ^b	26.29 ± 0.71a	13.02± 0.39 ^b	2.84 ± 0.17 ^a	0.60 ± 0.10 ^a						
	20–30	57.19 ± 1.43°	6.25 ± 0.96 ^a	12.74 ± 0.47 ^a	2.63 ± 0.19 ^a	1.18 ± 0.08 ^b						
2019												
	0–10	¹ 11.93 ± 0.47 ^a	45.13 ± 0.55 ^a	15.05 ± 0.41a	8.24 ± 0.29 ^a	19.65 ± 0.14 ^a	0.103ª	0.067a	45.90a	54.10a	0.582ª	
	10–20	12.15 ± 0.59 ^a	44.80 ± 1.07 ^a	15.20 ± 0.19 ^a	8.84 ± 0.47 ^b	19.01 ± 0.17 ^b	0.093b	0.054b	50.39b	49.61b	0.575°	
Control	20–30	10.49 ± 1.11 ^b	45.74 ± 0.89 ^b	15.04 ± 0.22a	9.35 ± 0.18°	19.38 ± 0.12°	0.089 ^b	0.051 ^b	51.14 ^b	48.86b	0.539 ^b	
Control I	0–10	"62.72 ± 1.58ª	23.51 ± 0.11a	11.66 ± 0.12a	1.82 ± 0.09 ^a	0.29 ± 0.08 ^a						
	10–20	62.79 ± 1.74 ^a	23.52 ± 0.27 ^a	11.40 ± 0.15 ^a	1.93 ± 0.11a	0.36 ± 0.08 ^a						
	20–30	61.04 ± 1.82 ^b	24.83 ± 0.18b	11.09 ± 0.17 ^b	2.22 ± 0.09b	0.82 ± 0.12b						
	0–10	116.68 ± 0.81a	47.04 ± 1.41 ^a	11.23 ± 0.36 ^a	7.09 ± 0.38 ^a	17.96 ± 0.28 ^a	0.102ª	0.066ª	37.97ª	62.03ª	0.647°	
	10–20	15.99 ± 1.19 ^b	45.94 ± 1.63 ^b	12.53 ± 0.69b	7.35 ± 0.51a	18.19 ± 0.14 ^a	0.102a	0.066a	39.69ª	60.31b	0.561 ^b	
Green manure	20–30	14.01 ± 0.63°	47.29 ± 0.87 ^a	12.64 ± 0.27 ^b	7.69 ± 0.17 ^b	18.37 ± 0.21a	0.100a	0.063a	41.48b	58.52°	0.539 ^t	
application	0–10	"63.56 ± 1.47ª	23.29 ± 0.15 ^a	9.56 ± 0.18a	3.07 ± 0.08a	0.52 ± 0.07°						
	10–20	55.74 ± 1.53 ^b	26.68 ± 0.43 ^b	12.63 ± 0.55 ^b	3.93 ± 0.14 ^b	1.02 ± 0.11a						
	20–30	52.91 ± 1.25°	28.55 ± 0.25 ^b	13.06 ± 0.29°	4.04 ± 0.11 ^b	1.44 ± 0.09 ^b						
				2	025							
	0–10	110.12 ± 0.31a	44.55 ± 1.07 ^a	16.29 ± 0.81a	8.12 ± 0.35 ^a	20.92 ± 0.82a	0.094ª	0.054ª	48.95ª	51.05ª	0.539	
	10–20	10.65 ± 0.44 ^a	45.02 ± 1.92 ^b	15.75 ± 0.52 ^b	8.13 ± 0.27 ^a	20.45 ± 0.65^{a}	0.085 ^b	0.047 ^b	51.93b	48.07b	0.567 ^t	
Control II	20–30	8.79 ± 0.59 ^b	45.53 ± 1.27 ^a	16.16 ± 1.05 ^a	8.64 ± 0.63 ^b	20.88 ± 1.03 ^a	0.084b	0.045b	52.06b	47.94b	0.477	
Control II	0–10	"69.32 ± 2.15ª	20.07 ± 0.56 ^a	9.36 ± 0.22a	1.11 ± 0.11 ^a	0.14 ± 0.09 ^a						
	10–20	68.23 ± 1.89 ^b	20.68 ± 0.55b	8.78 ± 0.29 ^b	1.98 ± 0.11 ^b	0.33 ± 0.10 ^a						
	20–30	68.42 ± 2.55 ^b	19.77 ± 0.63°	9.34 ± 0.37 ^a	2.05 ± 0.18°	0.42 ± 0.12 ^b						
	0–10	116.97 ± 1.04a	49.21 ± 0.74 ^a	10.67 ± 0.57 ^a	6.78 ± 0.44^{a}	16.37 ± 0.74 ^a	0.110a	0.077a	32.01ª	67.99ª	0.689	
Cross	10–20	17.31 ± 1.21 ^b	48.58 ± 1.02 ^b	12.05 ± 0.71 ^b	6.97 ± 0.28 ^b	15.09 ± 0.68 ^b	0.109ª	0.075ª	36.85b	63.15b	0.670°	
Green manure	20–30	16.78 ± 0.88 ^a	48.80 ± 1.12 ^b	12.17 ± 0.48 ^b	7.04 ± 0.56 ^b	15.21 ± 0.92 ^b	0.109ª	0.074ª	38.72°	61.28°	0.642b	
application II	0–10	"57.15 ± 1.41a	23.12 ± 0.17 ^a	15.03 ± 0.11 ^a	3.88 ± 0.08^{a}	0.82 ± 0.05^{a}						
·	10–20	50.45 ± 1.53 ^b	28.22 ± 0.19 ^b	15.67 ± 0.14 ^b	4.49 ± 0.05 ^b	1.17 ± 0.07 ^b						
	20–30	49.13 ± 1.62°	28.47 ± 0.18°	16.13 ± 0.17 ^a	4.82 ± 0.12°	1.45 ± 0.11 ^b						

Note: Indexed explanations of the experimental variants are fully provided in the captions to Table 2, and the decoding of indicators is described in the methodology section. I – indicators based on PSDA analysis results; II – indicators based on MACA analysis results. Different lowercase letters in the table indicate significant differences among treatments at the same soil layer (p < 0.05).

proportion of fractions in the 0.01–0.25 mm range by an average of 10.99% for the 0–30 cm soil layer, accompanied by a corresponding decrease in fractions in the 0.01–<0.001 mm range. In the absence of green manure or any fertilization, compared to the absolute control (2014), the changes showed an opposite trend.

This dynamic confirms a significant reduction in intra-fractional dispersion within the fraction range <0.001–0.25 mm due to the participation of organic components of the green manure mass during its decomposition in the soil. This aligns with the identified dispersity factor (Fd), which showed a stable decline from the beginning of the

experiment to the final assessment date in the paired comparison between the control and green manure variants, with an average annual gradient of 1.41% year⁻¹ for the 0–10 cm soil layer, 1.26% year⁻¹ for 10–20 cm, and 1.11% year⁻¹ for 20–30 cm.

Additionally, increases in the mean weight diameter of soil aggregates (MWD) and geometric mean diameter of soil aggregates (GWD) were observed in the 'Green manure application II' variant compared to 'Control II' by 24.71% and 54.79%, respectively. This corresponds positively with findings that optimization of the structuralaggregate state of the soil is accompanied by increases in both MWD and GWD indicators (Aksakal et al., 2020). These morphological structural changes in microaggregate soil fractions due to green manure application contributed to a significant increase in microaggregation dynamics, confirmed by the degree of incorporation of elementary soil particles into microaggregates (DI), which was on average 15.12% higher in the green manure variant for the 0-30 cm soil layer at the final assessment date compared to control. For the same comparison, an increase of 26.41% was noted in Fageler's structure factor (FSF).

Based on similar studies on the impact of bio-organic fertilization systems on soil microaggregate structure (Hu et al., 2020; Arel, 2021), it was established that the use of oilseed radish green manure created the prerequisites for microaggregation and a gradual increase in the proportion of 0.05-0.25 mm fractions. Considering the earlier mentioned characteristics of changes in the structural-aggregate composition at the 0.25-10.0 mm fraction level, green manure application shifts the distribution curve of fractions from a broad abscissa field with an ordinate peak at soil fractions greater than 7-10 mm to a narrower abscissa field with an ordinate peak in the 2 to 5 mm range. This occurs due to the noted process of organic carbonization of soil aggregates, which is more effective in terms of optimal dispersity based on physicochemical adsorption processes of organic carbon on the surface of soil particles and subsequent multistage aggregation (according to Wu et al., 2024).

Continuous organic matter accumulation in the soil over time will increase soil aggregates while simultaneously optimizing other soil properties—agrochemical, water, thermal, etc. The effectiveness and stability of such aggregation will be determined by the biochemical composition of the green manure biomass and the specifics of its biochemical transformation in the soil profile. This is confirmed by Qiang et al. (2024) and Stroud et al. (2024) and corresponds with the results on water stability of microaggregate fractions (Table 3, data index position II), which shows a pronounced dynamic decline from fractions 0.05–0.25 mm to fractions <0.001 mm.

The distribution of water-stable aggregates across microfraction ranges showed marked differences at the final assessment date when comparing the control and green manure variants. Specifically, in the 0-10 cm soil layer at the final date, a 16.41% decrease in the share of water-stable aggregates in the 0.05-0.25 mm fraction range was noted alongside increases of 6.43% in the 0.01-0.05 mm fraction, 6.45% in the 0.005-0.01 mm fraction, 2.68% in the 0.001-0.005 mm fraction, and 0.85% in the <0.001 mm fraction. Conversely, the 'Control II' variant, representing prolonged agricultural use without fertilization, showed an intensive increase in water-stable aggregates in the 0.25-0.05 mm fraction range with decreases in this parameter for other fractions. This agrees with earlier noted processes of increasing 1–<0.25 mm soil fractions in 'Control II' due to degradative destabilization associated with overall predicted decline in soil organic matter, which is identified as the primary aggregating factor for soil size fractions. Such dynamics, according to various studies (Teh, 2012; Qin et al., 2024; Park and Lee, 2025), will favor the formation of stable trends towards water-stable microaggregation, enhanced erosion resistance of soil horizons, and gradual optimization of soil agro-physical properties due to the growth of the largest fractions within the overall range of 0.25-< 0.0001 mm when oilseed radish is used as green manure. These generalizations are confirmed by the calculated indicators of the soil's structuralaggregate state (Table 4). The observed processes of increasing the proportion of water-stable aggregates (WSA) in the soil fraction interval series were consistently reflected in the overall increase in the total amount of water-stable aggregates.

A steady increase in this indicator was identified in the sequential monitoring series under the use of green manure (sideration). The average annual growth rate for the 0–30 cm soil layer over the entire research period, compared to the absolute control, was 1.10% per year, whereas the variant without sideration showed a general decline rate of 0.18% per year.

Table 4. Additional parameters for assessing the structural-aggregate state of the soil in experimental variants
based on the combined methods of dry and wet sieving (for the comparative period 2014–2025 for the basic soil
fraction range 0.25–10.0 mm)*

Experimental variant	Soil layer, cm	WSA, %	MWD _,	GMD, mm	MWD _{wet} ,	GMD _{wet} , mm	SSI	PSDI, %	PAD, %	SAI, %	SMal, %	MWAS, %	S _w	K-factor	FD	Cs	D, mm
	2014																
	0–10	49.01ª	2.53ª	1.96ª	0.65ª	0.33ª	0.26ª	74.28ª	46.29ª	35.80ª	21.38ª	26.04ª	74.28ª	0.078ª	2.62ª	1.94ª	35.92
Absolute control	10–20	48.12 ^b	2.52ª	1.98ª	0.65ª	0.33ª	0.26ª	74.33ª	47.66b	34.95 ^b	20.84ª	24.06b	74.33ª	0.082b	2.62ª	1.84 ^b	- 1
	20-30	47.55°	2.43b	1.93b	0.64ª	0.32ª	0.26a	73.60⁵	48.17°	34.19b	20.33b	21.78°	73.60b	0.071a	2.64b	1.60°	- 1
2019																	
	0–10	46.07ª	2.19ª	1.90ª	0.55ª	0.29ª	0.25ª	74.71ª	48.74ª	34.16ª	18.94ª	23.66ª	74.71ª	0.086ª	2.66ª	1.68ª	39.21
Control I	10–20	45.81ª	2.04b	1.82ª	0.51ª	0.28ª	0.25ª	74.81ª	49.24ª	33.19 ^b	17.99 ^b	22.80ª	74.81ª	0.088ª	2.66ª	1.57ª	-
	20–30	48.22b	2.02b	1.78b	0.60b	0.31ª	0.29b	70.55⁵	46.82b	34.49°	19.87□	20.94b	70.55⁵	0.080b	2.68b	1.42b	-
	0–10	52.22ª	2.95ª	2.17ª	0.80ª	0.38ª	0.27ª	72.82ª	43.72ª	38.27ª	24.66ª	26.71ª	72.82ª	0.056ª	2.55ª	2.39ª	31.74
Green manure application I	10–20	57.23b	2.94ª	2.22b	0.90 ^b	0.43 ^b	0.31 ^b	69.42b	38.54b	40.40 ^b	27.19 ^b	27.39b	69.42 ^b	0.051 ^b	2.59b	2.38ª	-
	20-30	59.54°	2.86 ^b	2.17ª	0.92 ^b	0.45 ^b	0.32 ^b	67.66°	36.15°	41.66°	28.46°	29.14°	67.66°	0.049b	2.60b	2.36ª	-
							2025	,						•			
	0-10 43.36° 1.97° 1.67° 0.49° 0.28° 0.25° 74.89° 50.60° 33.34° 17.69° 19.65° 74.89° 0.105°										0.105ª	2.74ª	1.48ª	45.66			
Control II	10–20	44.70b	1.96ª	1.66ª	0.49ª	0.28ª	0.25ª	75.21ª	49.15 ^b	33.17ª	17.62ª	20.25ª	75.21ª	0.102ª	2.72b	1.44ª	-
	20-30	46.02°	1.90 ^b	1.63 ^b	0.52ª	0.29ª	0.27ª	72.89b	47.71°	33.07ª	18.01ª	20.34ª	72.89b	0.100a	2.70b	1.29 ^b	-
	0–10	57.15ª	3.00a	2.28ª	0.97ª	0.45ª	0.32ª	67.69ª	38.18ª	43.12ª	29.65ª	30.66ª	67.69ª	0.049ª	2.52ª	2.76a	26.83
Green manure application II	10–20	61.30b	3.04 ^b	2.35b	1.07 ^b	0.50b	0.35⁵	64.69b	34.56b	44.68 ^b	31.82b	32.41 ^b	64.69b	0.044b	2.54b	2.77ª	-
application II	20-30	61.55b	3.01ª	2.38b	1.03 ^b	0.49b	0.34 ^b	65.72⁵	33.68°	44.12 ^b	31.10b	31.85b	65.72⁵	0.045b	2.55b	2.62b	-

Note: Indexed explanations of the experimental variants are fully provided in the captions to Table 2; the decoding of the indicators is in the Methods section. Different lowercase letters in the table indicate significant differences among treatments at the same soil layer (p < 0.05).

Within the analyzed soil layers, the maximum incremental gradient of 1.17% per year was recorded for the $20{\text -}30$ cm horizon, and the minimum -0.68% per year for the $0{\text -}10$ cm horizon, which confirms the conclusions of Talgre (2013) regarding the gradient of sideration effectiveness depending on the depth of incorporation of the green manure biomass into the soil profile. In this study, with a green manure incorporation depth of up to 16 cm and intensive tillage averaging 22.55 ± 6.31 cm during the $2014{\text -}2025$ period, the most significant impact on the soil was identified within the $14{\text -}25$ cm soil profile interval.

For the variants without sideration, the maximum decline gradient was observed in the 0–10 cm soil layer – 0.47% per year, gradually decreasing to 0.13% per year in the 20–30 cm soil layer. This distribution is supported by the evaluation of Medvedev et al. (2020), which indicated pronounced signs of soil cover degradation under maximal agrotechnological impact in the 0–15 cm soil layer.

It has been established (Aksakal et al., 2020; Dai et al., 2024; Poeplau et al., 2024) that

optimization of the structural-aggregate state of the soil, from the perspective of agronomically sound practice, results in higher values of MWD (mean weighted diameter) and GMD (geometric mean diameter) under both dry and wet sieving conditions (MWD_{wet}, GMD_{wet}). These conclusions are confirmed by the results of this study. Averaged over the 0-30 cm soil layer, MWD and GMD values under dry sieving at the final observation date in the sideration variant were 30.59% and 22.02% higher, respectively, compared to the absolute control variant, and 55.23% and 41.23% higher compared to the variant without sideration at the same observation date. Comparing the variant without sideration and the absolute control revealed a decrease in these indicators by 15.87% and 13.66%, respectively. Under wet sieving, while maintaining the same dynamics, more significant increases were identified for the sideration variant, with average coefficients of 1.32 for $\mbox{MWD}_{\mbox{\tiny wet}}$ and 1.24 for $\mbox{GMD}_{\mbox{\tiny wet}}.$ The MWD/GMD ratio also differed significantly: at the final observation date, it was 1.29 for the sideration variant and 1.18 for the variant without sideration. For

the wet sieving variant, these ratios were 2.13 and 1.76, respectively. Comparing the ratios MWD/ MWD_{wet} and GMD/GMD_{wet} for dry and wet sieving showed values of 2.95 and 3.89, and 4.87 and 5.84, respectively, for the corresponding experimental variants. Based on assessments by Zhou et al. (2020), Arel (2021), Li et al. (2024), and Dai et al. (2025), the lower value of this ratio for the mean weighted morphometric parameters of soil fractions indicates a consistent increase in the proportion of water-stable aggregates and enhancement of hydrophobic properties of soil aggregates in the sideration variant, as well as an overall optimization of soil dispersion. This positively correlates with the potential structural deformation index (PSDI), which for the 0-30 cm soil layer decreased by 8.13% in the sideration variant at the final observation date compared to the absolute control, confirming, based on Ding and Zhang (2016), a gradual and stable process of restoring agronomically valuable soil structure.

These conclusions were also confirmed by the value of the soil stability index (SSI), which is considered an identifier of the overall water stability of soil aggregates, as it determines their weighted average morphometry after wet sieving compared to the analogous morphometry after dry sieving (Franzluebbers et al., 2022). This indicator, across the variants, demonstrates a consistent cumulative increase in the treatments with green manure at all observation dates, with a growth coefficient of up to 1.31 relative to the variant without green manure at the final observation date.

It should be noted that in the control variants without green manure, the formation of SSI was specific. Throughout the study period, this indicator showed relative stability with an average value for the 0-30 cm soil layer at the level of 0.26–0.27. However, this pattern resulted from an increase in its value in the 20-30 cm soil layer and a decrease in the 0-20 cm soil layer. The identified dynamics of decreasing MWD with depth, against the opposite increase of MWDwet, indicate internal profile processes of eluviation with the displacement of soil particles having a high potential deformation index (DI) to the lower horizons of the profile. For the variants with green manure, this pattern gradually changes with the increasing duration of the green manure practice, shifting the maximum SSI value to the 10-20 cm soil horizon. These processes are also confirmed by the composite indicator mean weight

aggregate stability (MWAS), which combines the morphometry of soil aggregates and their water stability in a single interrelated complex.

In the 'Control II' variant at the final observation date, compared to the initial control variant, a decrease in this indicator by 11.72% was noted, against its increase in the 'Green Manure Application I' variant under the same comparison by 39.26%. Considering the research results of Aksakal et al. (2020), this confirms the previously identified stable processes in the green manure variants of predominantly forming soil aggregate fractions in the 3–7 mm range, with a significant increase in their water stability. As a result, due to the defined high direct correlation (r = 0.853, p < 0.01) between MWAS and SSI indicators, a simultaneous positive effect in optimizing both the structural-aggregate composition of soils and the proportion of water-stable aggregates is confirmed through the consistent use of oilseed radish as green manure.

Furthermore, based on the studies of Hu et al. (2018) and Xu et al. (2024), this pattern of formation confirms the property of green manure to optimize not only the structural-aggregate state of the soil but also to influence the complex hydrophysical properties and processes of soil particle movement in a unified system with corresponding vectors and intensities of moisture movement through the soil profile. Green manure allowed localization and optimization of this process, reducing the sensitivity of soil aggregates to moisture redistribution within the soil profile, especially under conditions of excessive intensive wetting, and particularly its consequences in variants of intra-profile infiltration. These results are supported by values of indicators such as Susceptibility of Soil to Wetting (Sw) and Erodibility (K-factor), which showed minimal values overall for the 0–30 cm soil layer (with a maximum in the 10–20 cm layer) in the 'Green Manure Application II' variant. At the same time, the overall reduction of these indicators compared to the 'Control II' variant averaged 11.16% and 55.05% for the 0-30 cm soil layer, respectively.

Considering that the Sw indicator identifies the impact of water on soil aggregate breakdown in terms of increasing their miniaturization degree (Klíč, 2024), and the erodibility (K-factor) determines soil erosion resistance (Ding and Zhang, 2016; Tian et al., 2022; Li et al., 2024), green manure ensured a significant optimization

of the resistance potential of the upper horizons of the soil profile against destruction by atmospheric precipitation and downward water flow.

The application of green manure had a positive effect on a complex of indicators that determine the degree of soil layer structuring (stable aggregates index (SAI), stable macroaggregates index (SMaI), fractal dimension (FD)), as well as the degree of expression of this structuring in terms of its potential reduction under the influence of water and compaction (PSDI and PAD) (Table 4). Specifically, on average for the 0–30 cm horizon, the SAI increased by 9.79% in the 'Green Manure Application II' variant compared to the 'Absolute Control' variant, while the SMaI increased by 11.22%, simultaneously with a reduction in these values in the variant without green manure by 1.00% and 1.87%, respectively.

According to the gradation classification of land categories by Márquez et al. (2004), based on the recorded values of SAI and SMaI, the soil cover in the 'Green Manure Application II' variant - with values greater than 35% for both indicators - corresponds to the 'Cropped system' category with a pronounced soil rehabilitation process. For the 'Control II' variant, with indicator values less than 35% and 20%, respectively, the soil cover corresponded to the 'Cropped system' category exhibiting signs of soil agro-physical degradation. At the same time, green manure significantly reduced soil aggregate destruction according to the proportion of aggregate destruction (PAD) index - its value was minimal precisely in the green manure variant, averaging 35.47% for the 0-30 cm soil layer, which was 12.99% lower than in the absolute control variant and 13.68% lower than in the 'Control II' variant. According to Kemper and Rosenau (1986), such dynamics indicate intensification of the soil aggregation process, especially in the 10-30 cm soil layer, which confirmed earlier conclusions by Talgre (2013) regarding the localized intensifying effect of the green manure biomass.

Regarding the fractal dimension (FD) of the soil structural-aggregate state, the average value for the 0–30 cm soil layer in the 'Green Manure Application II' variant was 4.28% lower compared to the absolute control and 6.41% lower than in the 'Control II' variant. Based on a series of analytical evaluations (Pirmoradian et al., 2005; Lawal, 2022), this proves the positive influence of green manure application on reducing the overall variability of soil aggregate

morphometry, forming a more uniform soil dispersed environment, and the anticipated associated optimization of derivative agrophysical indicators.

In summary, the positive shifts in the formation of the structural-aggregate state of the soil in variants with oilseed radish green manure positively influenced the widely used soil science indicator – the coefficient of structurality (Cs). This indicator increased more than 1.6 times in the green manure variants at the final observation date relative to the absolute control. According to the gradation of this indicator (Medvedev et al., 2020), the 'Green Manure Application II' variant reached a Cs level corresponding to good conditions (Cs > 2.0), while the 'Control II' variant showed satisfactory conditions (Cs < 1.5). These formation features are clearly illustrated by the data in Figure 6.

The optimization state of the arable horizon soil profile structure was additionally confirmed by digital processing of soil surface images after the respective tillage treatment, using the separation length criterion of soil structural aggregates (D) (Figures 7–8).

It was established that the consistent use of green manuring with oilseed radish levels the morphometry of soil aggregates in the topsoil layer during identification after early spring tillage at the state of physical maturity. This nearly halves the range of interval grouping of soil aggregates according to the D criterion, reduces the overall variability of morphometry (as measured by the coefficient of variation, C.) by 13.89%, and decreases the average D value for the identified aggregate population by 1.7 times. These results positively correlate with the identified trends in soil fraction formation according to PSDA analysis and the observed dynamics in the formation of the FD indicator of the soil's structural-aggregate state.

The system of allelopathic adaptive mechanisms of oilseed radish, in terms of its influence both on subsequent crops and on soil phytotoxicity (Tsytsiura, 2022; Tsytsiura and Sampietro, 2024), has necessitated an assessment of the agrobiological and agroecological feasibility of the long-term use of oilseed radish green manure on the same field based on the criterion of phytotoxicity. The results of this assessment are presented in Figure 9. According to the presented data, the green biomass of oilseed radish is classified as a plant component

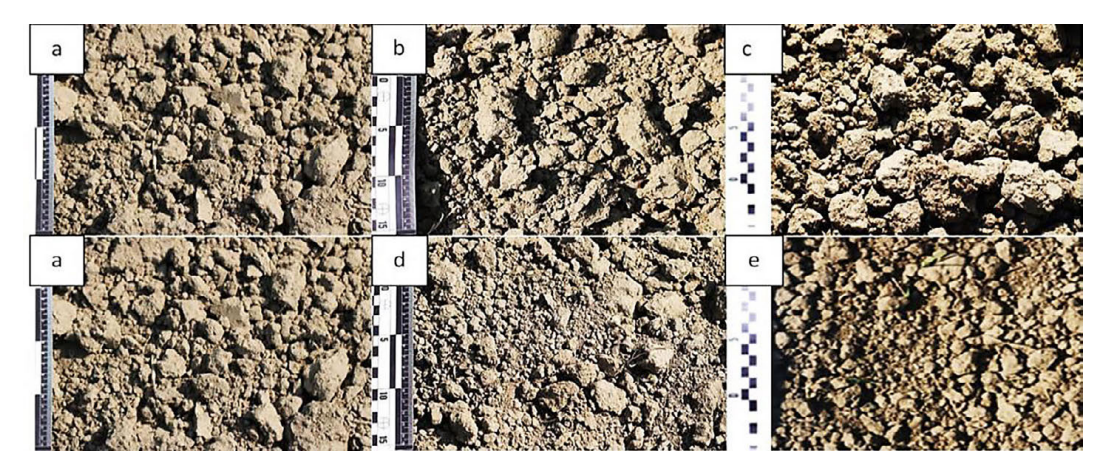


Figure 6. Soil surface condition on the third day after early spring disking to a depth of 10–12 cm depending on the experimental variants, 2014–2025. **Note:** a – Absolute Control (2014); b – Control I (2019); c – Green Manure Application I (2019); d – Control II (2025); e – Green Manure Application II (2025)

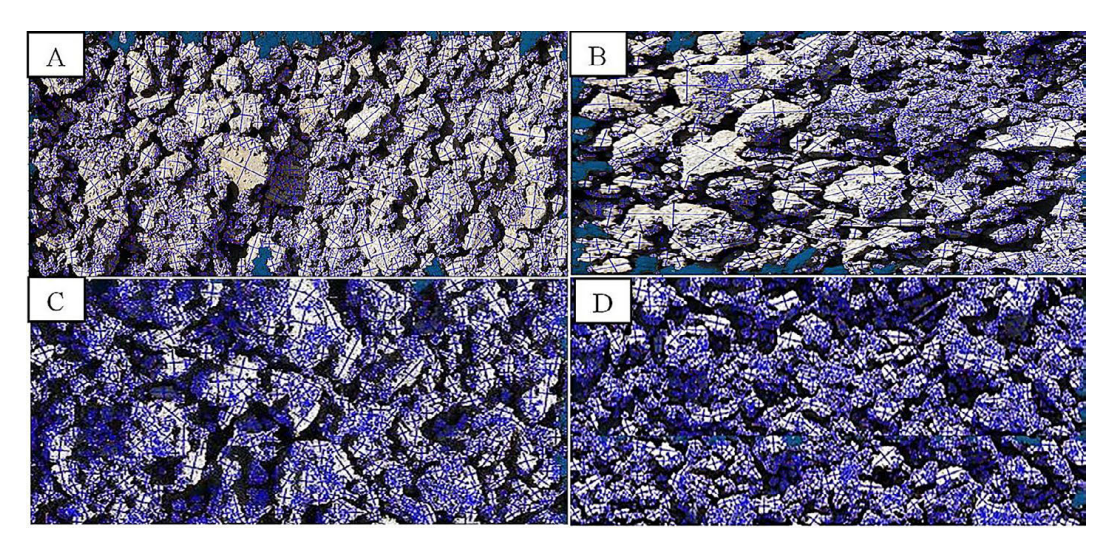


Figure 7. Results of morphometric determination of soil aggregates using the BaseGrain v. 2.2.0.4 software based on the separation length criterion of soil structural aggregates (D, mm) on frontal images of the soil surface after spring disking to a depth of 10–12 cm (Position A – experimental variant 'Control I',

Position B – variant 'Control II', Position C – variant 'Green manure application I',

Position D – variant 'Green manure application II'; blue lines of vertical and horizontal orientation on soil aggregates indicate the axes as linear parameters of the Feret diameter (Figure 1))

with a relatively high level of allelopathic activity, which positively correlates with its established biofumigation potential (Duff et al., 2020; Tsytsiura, 2024a) and with the evaluation of allelopathically active compounds in the leaf-stem biomass of cruciferous species (Grodzinsky, 1973; Almhemed and Ustuner, 2023). These features contributed to an overall increase in soil phytotoxicity based on its biotesting.

It was determined that under the systematic use of oilseed radish green manure, soil phytotoxicity increased both in the control treatment without green manuring and in the treatment with its application, although the rates of increase differed significantly. On average, for the 0–30 cm soil layer, the increase in phytotoxicity during the comparison period of the reference dates was 0.116 CCU (conditional coumarin units) year⁻¹ in the control treatment, while under systematic green manuring it was 0.281 CCU year⁻¹. The dynamics of phytotoxicity increase in the control treatment can be explained by the conclusions of Ohno et al. (2000), regarding the general decrease in the rate of plant residue immobilization against the background of identified soil

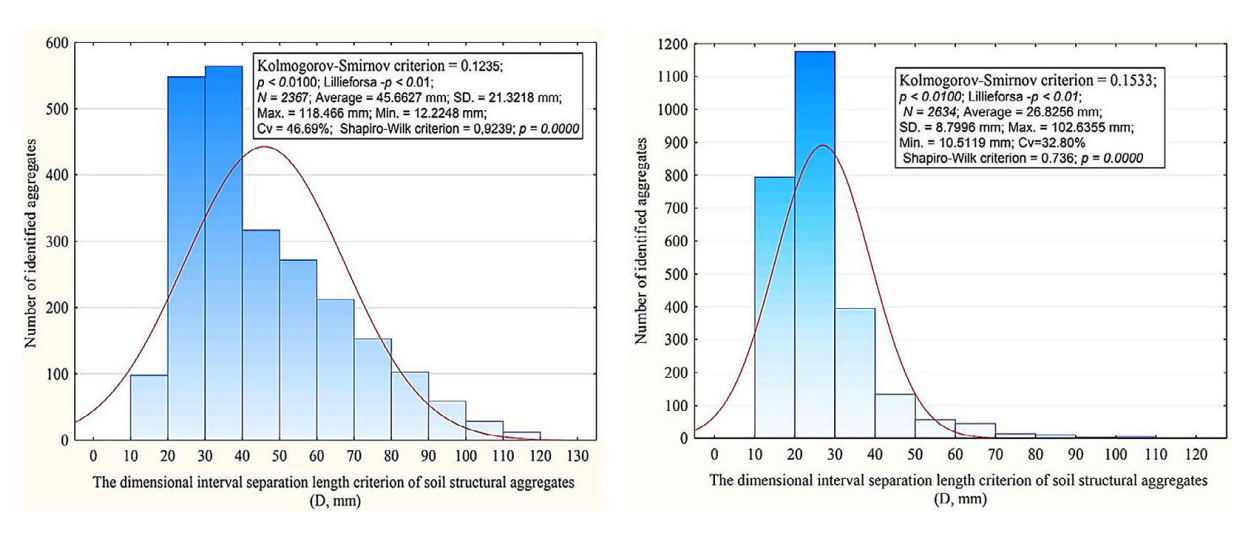


Figure 8. Results of statistical clustering of the identification of the separation length criterion of soil structural aggregates (D, mm) on frontal photographs of the soil surface after spring disking to a depth of 10–12 cm in 2025 (left position – 'Control II' experimental variant, right position – 'Green manure application II' experimental variant)

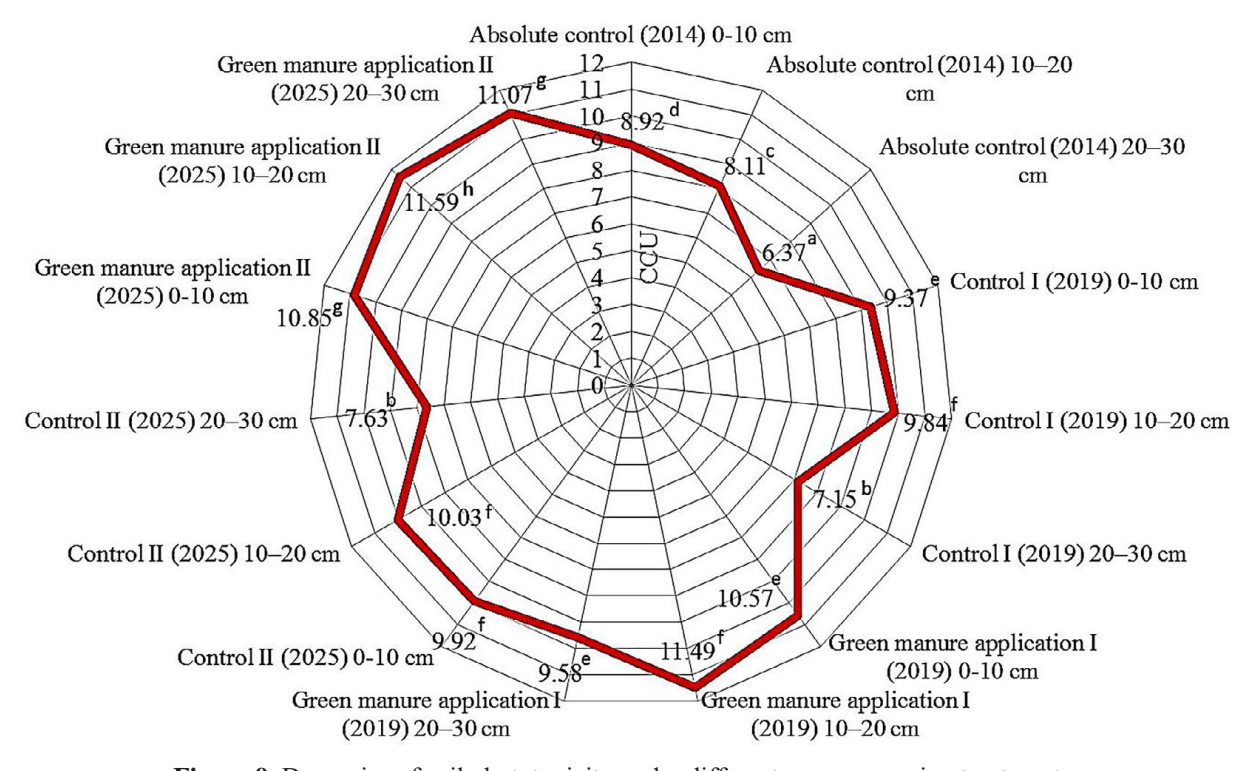


Figure 9. Dynamics of soil phytotoxicity under different green manuring treatments, conditional coumarin units (CCU) (2014–2025). **Note:** Explanations of experimental treatments are provided in the footnotes of Table 2. Different lowercase letters indicate significant differences among treatments within the same soil layer (p < 0.05)

degradation, the accumulation of plant residues with a low decomposition rate, and the creation of prerequisites for an overall rise in soil phytotoxicity. According to Grodzinsky (1973), a phytotoxicity level of 20 CCU is critical in terms of significantly affecting not only the germination of subsequent crops but also the

overall growth processes at the early stages of their vegetation. Based on this, the applied green manuring regime (once every two years), with an attainable average level of 11.17 CCU in the 0–30 cm soil layer, allows for agronomically acceptable rates of soil phytotoxicity increase while maintaining a positive effect on soil

agrophysical properties, and can therefore be recommended for gray forest soils. In contrast, annual systematic application of oilseed radish green manure on the same field, according to Grodzinsky (1991), is highly likely to lead to a substantial increase in phytotoxicity, exceeding the 20 CCU threshold. Once again, drawing on the assessments of Tiquia et al. (1996) for soils of a different type and under alternative intensities of green manuring, this issue requires further investigation.

CONCLUSIONS

Systematic use of green manure in grainrow crop rotations on gray forest soils under conditions of unstable moisture, compared to the variant without green manure over a longterm period, ensured positive changes in the complex of aggregate-structural soil parameters. The main changes included a positive increasing average comparable dynamic for the 0-30 cm soil layer in the share of agronomically valuable structure, 0.25-10.0 mm CAVS by 9.04%, the share of water-regulating fractions, 1.0-3.0 mm CWRF by 3.31%; the share of wind-resistant aggregates >1 mm CWRA by 4.56%, and the share of water-stable aggregates by 13.19%, accompanied by increases in the soil stability index by 1.3 times, stable aggregates index by 1.29 times, stable macroaggregates index by 1.57 times, and the coefficient of structurality by 1.67 times. These changes enhanced soil erosion resistance due to nearly a twofold reduction in the erodibility factor (K-factor), stabilized the spatial morphometry of soil aggregates by reducing the Fractal Dimension criterion of the soil structural state by 4.28%, and the separation length criterion of soil structural aggregates by 1.7 times. As a result, green manure application achieved the formation of an optimized structuralaggregate state of the arable soil horizon with an overall reduction of multifactorial destruction of soil aggregates by 12.99% according to the comprehensive criterion proportion of aggregate destruction (PAD).

Given the overall positive effect on the complex of soil agrophysical parameters, the feasibility of applying oilseed radish green manuring once every two years on the same field has been demonstrated.

REFERENCES

- Abdelrahman M., Wang W., Lv H., Di Z., An Z., Lijun W., Shaukat A., Bo W., Guangsheng Z., Liguo Y., Guohua H. (2022). Evaluating the effect of forage rape (*Brassica napus*) ensiling kinetics on degradability and milk performance as nonconventional forage for dairy buffalo. *Frontiers* in Veterinary Science, 9, 926906. https://doi. org/10.3389/fvets.2022.926906
- 2. Abdulraheem, M.I., Tobe O.K. (2022). Green manure for agricultural sustainability and improvement of soil fertility. *Farming & Management* 7, 1–8. https://doi.org/10.31830/2456-8724.2022.FM-101
- 3. Aksakal E.L., Angin I., Sari S. (2020). A new approach for calculating aggregate stability: Mean weight aggregate stability (MWAS). *Catena*, 194, 104708. https://doi.org/10.1016/J. CATENA.2020.104708
- Almhemed K., Ustuner T. (2023). Assessment of allelopathic influence of some cruciferous species on germination indicators of field dodder seeds. *Advances in Weed Science*, 41, e020230048. https://doi.org/10.51694/AdvWeedSci/2023;41:00029
- Arel, C. M. (2021). Cover Crop Effects on Near-Surface Soil Aggregate Stability in the Southern Mississippi Valley Loess (MLRA 134). Crop, Soil and Environmental Sciences Undergraduate Honors Theses Retrieved. University of Arkansas. Department of Crop, Soil, and Environmental Sciences.
- Bieganowski A., Ryżak M. (2011). Soil Texture: Measurement Methods. In: Gliński, J., Horabik, J., Lipiec, J. (eds) Encyclopedia of Agrophysics. Encyclopedia of Earth Sciences Series. Springer. https://doi.org/10.1007/978-90-481-3585-1_157
- Bulgakov V., Kaletnik H., Trokhaniak O., Lutkovska S., Klendii M., Ivanovs S., Popa L., Yaropud V. (2023). Investigation of the energy indicators for the surface treatment of soil by a harrow with a screw-type working body. *INMATEH-Agricultural Engineering*, 71(3), 818–833. https://doi.org/10.35633/inmateh-71-72
- Butenko Y., Rudska N., Kovalenko N., Hotvianska A., Horshchar V., Tkachenko R., Turchina S., Dashutina L., Mikulina M., Toryanik V. (2025). The impact of environmentally balanced agricultural systems on changes in the agrophysical state of typical chernozem soil and the energy management of sunflower cultivation. *Journal of Ecological Engineering*, 26(7), 428–437. https://doi.org/10.12911/22998993/203917
- 9. Church M.A., McLean D.G., Wolcott J.F. (1987). River bed gravels: Sampling and analysis. Sediment transport in gravel-bed rivers, CR Thorne, JC Bathurst, RD Hey, eds., Wiley, Chichester, U.K., 43–88.

- 10. Dai W., Feng G., Huang Y., Adeli A., Jenkins J. N. 2024. Influence of cover crops on soil aggregate stability, size distribution and related factors in a no-till field. Soil & Tillage Research 244, 106197. https://doi.org/10.1016/j.still.2024.106197
- Dai W., Adeli A., Huang Y., Feng G., Jenkins J. N. (2025). Soil aggregate stability and erodibility as influenced by soil amendments and winter cover crop in upland soils. *Soil Science Society of America Journal*, 89(1). https://doi.org/10.1002/saj2.70022
- 12. Ding, Wf., Zhang, Xc. (2016). An evaluation on using soil aggregate stability as the indicator of interrill erodibility. *Journal of Mountain Science 13*, 831–843. https://doi.org/10.1007/s11629-015-3447-4
- 13. Duff J., van Sprang C., O'Halloran J., Hall Z. (2020). Guide to Brassica Biofumigant Cover Crops Managing soilborne diseases in vegetable production systems. Horticulture Innovation through VG16068. State of Queensland.
- 14. DSTU ISO 11277:2005. (2005). Soil quality. Determination of the particle size distribution of soil mineral material. Sieving and sedimentation method (ISO 11277:1998, IDT). (in Ukrainian).
- 15. Franzluebbers A. J. (2022). Soil mean-weight diameter and stability index under contrasting tillage systems for cotton production in North Carolina. Soil Science Society of America Journal, 86, 1327–1337. https://doi.org/10.1002/saj2.20458
- Gentsch N., Riechers F., Boy J., Schwenecker D., Feuerstein U., Heuermann D., Guggenberger G. (2024). Cover crops improve soil structure and change organic carbon distribution in macroaggregate fractions. *Soil*, 10, 139–150. https://doi. org/10.5194/soil-10-139-2024
- 17. Green Manure Global Market Report 2024. (2023). By Type (Leguminous, Non Leguminous), By Source(Dhaincha, Sesbania, Sunhemp, Other Sources), By Application(Grains And Cereals, Pulses And Oilseeds, Fruits And Vegetables, Other Applications) Market Size, Trends, And Global Forecast 2024–2033. URL: https://www.thebusinessresearchcompany.com/report/green-manure-global-market-report
- 18. Grodzinsky A.M. (1973). *The Basis of Chemical Plant Interactions*. Naukova Dumka Kiev. 205 (in Russian).
- 19. Grodzinsky A.M. (1991). *Allelopathy of Plants and Soil Exhaustion*. Naukova Dumka Kiev, 432 (in Russian)
- 20. Hansen V., Müller-Stöver D., Magid J. (2022). *Green manure crops for low fertility soils*. https://orgprints.org/id/eprint/37832/1/poster_Veronika%20Hansen.pdf (date of application 25.06.2025).
- 21. Hu X., Chen J., Zhu L. (2020). Soil aggregate size distribution and stability of farmland

- as affected by dry and wet sieving methods. *Zemdirbyste-Agriculture*. *107*, 179–184. https://doi.org/10.13080/z-a.2020.107.023
- 22. Hu B., Wang Y., Wang B., Wang Y., Liu C., Wang C. (2018). Impact of drying-wetting cycles on the soil aggregate stability of Alfisols in southwestern China. *Journal of Soil and Water Conservation* 73(4), 469–478. https://doi.org/10.2489/jswc.73.4.469
- 23. ISO 10930:2012. (2012). Soil quality –Measurement of the stability of soil aggregates subjected to the action of water. URL: https://www.iso.org/standard/46433.html (date of application 25.06.2025).
- 24. Jia Q., Zheng H., Shi Z., Liu X., Sun D., Zhang J. (2024). Effects of straw and green manure addition on crop yield, soil properties and CH4 emissions: A meta-analysis. *Agronomy*, 14, 2724. https://doi.org/10.3390/agronomy14112724
- Kaletnik G., Lutkovska S. (2020). Strategic priorities of the system modernization environmental safety under sustainable development. *Journal of Environmental Management and Tourism 11*, 5(45), 1124–1131. https://doi.org/10.14207/ejsd.2021.v10n1p81
- 26. Kemper W., Rosenau R. (1986). *Aggregate stability and size distribution*. (In) Methods of Soil Analysis Part I, 2nd Ed. p. Klute A (Ed). ASA and SSSA, Madison WI, 425–442.
- 27. Klíč I. R. (2024). Conceptual model of the land-use influence on representation of water-stable aggregates in topsoil. Ph.D. Thesis. Czech University of Life Sciences Prague. Department of Landscape and Urban Planning.
- 28. Kopittke P.M., Menzies N.W., Wang P., McKenna B.A., Lombi E. (2019). Soil and the intensification of agriculture for global food security. *Environment International 132*, 105078. https://doi.org/10.1016/j.envint.2019.105078
- 29. Lawal H. M. (2022). Application of fractal theory in quantifying soil aggregate stability as influenced by varying tillage practices and cover crops in northern guinea savanna, Nigeria. *Tropical and Subtropical Agroecosystems* 25, 025. https://doi.org/0.56369/tsaes.3878
- 30. Le Bissonnais Y. (2016). Aggregate stability and assessment of soil crustability and erodibility: i. theory and methodology. *European Journal of Soil Science*, 67(1), 11–21. https://doi.org/10.1111/ejss.4_12311
- Lee C.-R., Kim S.H., Oh Y., Kim Y.J., Lee, S.-M. (2023). Effect of green manure on water-stable soil aggregates and carbon storage in paddy soil. *Korean Journal of Soil Science and Fertilizer*, 56(2), 191–198. https://doi.org/10.7745/KJSSF.2023.56.2.191
- 32. Lei B., Wang J., Yao H. (2022). Ecological and environmental benefits of planting green manure in paddy fields. *Agriculture*, *12*(2), 223. https://doi.org/10.3390/agriculture12020223

- 33. Li Y., Jia X., Zhao W., Gao R., Luo W., Wang T. (2025). Changes in soil aggregates and aggregate-associated carbon following green manure-maize rotations in coastal saline soil. *Agronomy*, *15*(6), 1283. https://doi.org/10.3390/agronomy15061283
- 34. Li M., Wang K., Ma X., Fan M., Song Y. (2024). effects of land use change on soil aggregate stability and erodibility in the Karst Region of Southwest China. *Agronomy* 14(7), 1534. https://doi.org/10.3390/agronomy14071534
- 35. Liu X.H., Zhou X., Deng L.C., Fan L.Y., Qu L., Li M. (2020). Decomposition characteristics of rapeseed green manure and effect of nutrient release on soil fertility. *Hunan Agricultural Science*, *416*, 39–44.
- 36. Lutkovska S., Kaletnik G. (2020). Modern organizational and economic mechanism for environmental safety. *Journal of Environmental Management and Tourism*, 11, 3(43), 606–612. https://doi.org/10.14505/jemt.11.3(43).14
- 37. Ma D., Yin L., Ju W., Li X., Liu X., Deng X., Wang S. (2021). Meta-analysis of green manure effects on soil properties and crop yield in Northern China. *Field Crops Research*, *266*, 108146. https://doi.org/10.1016/j.fcr.2021.108146
- 38. Márquez C. O., Cambardella C. A., Elliott E. T. (2004). Aggregate size stability distribution and soil stability. *Soil Science Society of America Journal* 68(3), 725–735. https://doi.org/10.2136/sssaj2004.7250
- 39. Mbagwu J. S. C., Bazzoffi P. (1989). Properties of soil aggregates as influenced by tillage practices; *Soil Use and Management 5*, 180–188. https://doi.org/10.1111/j.1475-2743.1989.tb00781.x
- 40. Medvedev V.V., Plisko I.V., Krylach S.I., Nakisko S.G., Uvarenko K.Y. (2020). *Physical degradation of arable soils of Ukraine (assessment, prevention, suspension)*. Kharkiv: NSC "A. N. Sokolovsky Institute of Soil Science and Agrochemistry". (in Ukrainian).
- 41. Meng X., Wang B., Zhang X., Liu C., Ji J., Hao X., Yang B., Wang W., Xu D., Zhang S., Wang X., Cao M., Wang Y. (2025). Long-term crop rotation revealed the relationship between soil organic carbon physical fraction and bacterial community at aggregate scales. *Microorganisms* 13, 496. https://doi.org/10.3390/microorganisms13030496
- 42. Nurhartanto N., Zulkarnain Z., Wicaksono A. A. (2022). Analysis of several soil physical properties as indicators of soil degradation in dry land. *Jurnal Agroekoteknologi Tropika Lembab*, 4(2), 107–112.
- 43. Ohno T., Doolan K., Zibilske L.M., Liebman M., Gallandt E.R. Berube C. (2000). Phytotoxic effects of red clover amended soils on wild mustard seedling growth. *Agriculture, Ecosystems &*

- Environment, 78, 187-192. https://doi.org/10.1016/ S0167-8809(99)00120-6
- 44. Park S., Lee J.-G. (2025). Green manure improves humification and aggregate stability in paddy soils. *Soil Biology and Biochemistry* 206, 109796. https://doi.org/10.1016/j.soilbio.2025.109796
- 45. Peng J., Xiao L., Xu Z., Chen B., Zhou G., Qiao C., Wu, Z. (2024). Effects of different land use change on soil aggregate and aggregate associated organic carbon: a meta-analysis. *Polish Journal of Environmental Studies 33*(5), 5263–5274. https://doi.org/10.15244/pjoes/183084
- 46. Pirmoradian N., Sepaskhah A.R., Hajabbasi M.A. (2005). Application of fractal theory to quantify soil aggregate stability as influenced by tillage treatments. *Biosystems Engineering 90*(2), 227–234. https://doi.org/10.1016/j.biosystemseng.2004.11.002
- 47. Poeplau C., Riefling T., Schiedung M., Anlauf R. (2024). Land use and soil property effects on aggregate stability assessed by three different slaking methods. *European Journal of Soil Science*, 75(4), e13549. https://doi.org/10.1111/ejss.13549
- 48. Pons L.J., Zonneveld I.S. (1965). Soil ripening and soil classification; initial soil formation in alluvial deposits with a classification of the resulting soils. ILRI Publication 13, Wageningen.
- 49. Qiang M., Zhang X., Zhuang X., Zhang H. (2024). Effect of organic amendment and mineral fertilizer on soil aggregate stability and maize yield on the Loess Plateau of China. *Polish Journal of Environmental Studies 33*(3), 2255–2265. https://doi.org/10.15244/pjoes/174782
- 50. Qin W., Wang K., Min K., Zhang Y., Wang Z., Liu X. (2024). Agricultural land abandonment promotes soil aggregation and aggregate-associated organic carbon accumulation: A global meta-analysis. *Plant Soil* 503, 629–644. https://doi.org/10.1007/s11104-024-06609-7
- Rezá cová V., Czakó A., Stehlík M., Mayerová M., Šimon T., Smatanová M., Madaras M. (2021). Organic fertilization improves soil aggregation through increases in abundance of eubacteria and products of arbuscular mycorrhizal fungi. *Scientific Reports 11*, 12548. https://doi.org/10.1038/s41598-021-91653-x
- 52. Singh D., Devi K.B., Ashoka P., Bahadur R., Kumar N., Devi O. R., Shahni Y.S. (2023). Green manure: aspects and its role in sustainable agriculture. *International Journal of Environment and Climate Change*, 13(11), 39–45. https://doi.org/10.9734/ijecc/2023/v13i113142
- 53. Stähly S., Friedrich H., Detert M. (2017). Size ratio of fluvial grains' intermediate axes assessed by image processing and square-hole sieving. *Journal of Hydraulic Engineering 143*, 1–6. https://doi.org/10.1061/(ASCE)HY.1943-7900.0001286

- 54. Stoyan D, Unland G. (2022). Point process statistics improves particle size analysis. *Granular Matter*, 24, 115. https://doi.org/10.1007/s10035-022-01278-8
- 55. Stroud J. L., Kemp S. J., Sturrock C. J. (2024). The effect of organic matter amendments on soil surface stability in conventionally cultivated arable fields. *Soil Use and Management 40*, e12985. https://doi.org/10.1111/sum.12985
- 56. Talgre L. (2013). Biomass production of different green manure crops and their effect on the succeeding crops yield. PhD Thesis. Institute of Agricultural and Environmental Sciences Estonian University of Life Sciences. Tartu.
- Teh C. B. S. (2012). The stability of individual macroaggregate size fractions of ultisol and oxisol soils.
 Journal of Agriculture, Science and Technology 14, 459–466.
- 58. Test Guidelines for the conduct of tests for distinctness, uniformity and stability of Fodder Radish (*Raphanus sativus* L. var. *oleiformis* Pers.). 2017. TG/178/3, UPOV, Geneva.
- 59. Tian S., Zhu B., Yin R., Wang, M.W., Jiang Y.J., Zhang C.Z., Li D.M., Chen X.Y., Kardol P., Liu M.Q. (2022). Organic fertilization promotes crop productivity through changes in soil aggregation. *Soil Biology and Biochemistry 165*, 108533. https:// doi.org/10.1016/j.soilbio.2021.108533
- 60. Tiquia S.M., Tam N.F.Y., Hodgkiss I.J. (1996). Effects of composting on phytotoxicity of spent pig-manure sawdust litter. *Environmental Pollution*, *93*(3), 249–256. https://doi.org/10.1016/S0269-7491(96)00052-8
- 61. Tokarchuk D., Pryshliak N., Berezyuk S., Tokarchuk O. (2024). Advancing sustainable reconstruction in Ukraine after full scale invasion: utilizing a "green" economic approach and essential guidelines for successful implementation. *Polityka Energetyczna* 27(2), 71–88. https://doi.org/10.33223/epj/185209
- 62. Toungos M.D., Bulus Z.W. (2019). Cover crops dual roles: Green manure and maintenance of soil fertility, a review. *International Journal of Innovative Agriculture and Biology Research*, 7(1), 47–59.
- 63. Tsytsiura, Y.H. (2020). Modular-vitality and ideotypical approach in evaluating the efficiency of construction of oilseed radish agrophytocenosises (*Raphanus sativus* var. *oleifera* Pers.). *Agraarteadus*, *31*(2), 219–243. https://doi.org/10.15159/jas.20.27
- 64. Tsytsiura Y.H. (2022). Estimation of species allelopathic susceptibility to perennial weeds by detailing the formation period of germinated seeds of oilseed radish (*Raphanus sativus* L. var. *oleiformis* Pers.) as the test object. *Agraarteadus*, 33(1), 176–191 https://doi.org/10.15159/jas.22.09

- 65. Tsytsiura Y. (2023). Possibilities of using FijiImagej2, WipFrag and BASEGRAIN programs for morphometric and granulometric soil analysis. *Engenharia Agrícola, Jaboticabal, 43*(6), e20230101. http://dx.doi.org/10.1590/1809-4430-Eng.Agric.v43n6e20230101/2023
- 66. Tsytsiura, Y. (2024a). Evaluation of Ecological Adaptability of Oilseed Radish (*Raphanus sativus* L. var. *oleiformis* Pers.) Biopotential realization in the system of criteria for multi-service cover crop. *Journal of Ecological Engineering*, 25(7), 265–285. https://doi.org/10.12911/22998993/188603
- 67. Tsytsiura Y. (2024b). Potential of oilseed radish (*Raphanus sativus* l. var. *oleiformis* Pers.) as a multiservice cover crop (MSCC). *Agronomy Research*, 22(2), 1026–1070. https://doi.org/10.15159/AR.24.086
- 68. Tsytsiura Y. (2025). Ecological adaptive tactics of oil radish root formation at different terms of green manure application. *Journal of Ecological Engineering*, 26(9), 420–439. https://doi.org/10.12911/22998993/205413
- 69. Tsytsiura Y., Narwal S.S. (2025). USSR Prominent Allelopathy Scientists Part III (1926-2010). *Allelopathy Journal*. 2025. Vol. 65. №2. P. 111–146. https://doi.org/10.26651/allelo.j/2025-65-2-1535
- Tsytsiura Y., Sampietro D. (2024). Allelopathic effects of annual weeds on germination and seedling growth of oilseed radish (*Raphanus sativus* L. var. *oleiformis* Pers.). *Acta Fytotechnica et Zootechnica*, 27(1), 77–97. https://doi.org/10.15414/afz.2024.27.01.77-97
- 71. Usman S., Jayeoba J.O. (2025). Evaluation of soil structural quality and soil fertility indicators of dryland and fadama milieus based on soil profile description at 0–20 cm soil depth. *Discover Soil* 2, 24. https://doi.org/10.1007/s44378-025-00049-0
- 72. Wong J. (2018). *Handbook of Statistical Analysis and Data Mining Applications* (Second Edition). Academic Press.
- 73. Wu J., Teng B., Zhong Y., Duan X., Gong L., Guo W., Qi P., Haider F. U., Cai L. (2024). Enhancing Soil Aggregate Stability and Organic Carbon in Northwestern China through Straw, Biochar, and Nitrogen Supplementation. *Agronomy* 14(5), 899. https://doi.org/10.3390/agronomy14050899
- 74. Xingming Z., Lei L., Chunmei W., Leran H., Tao J., Xiaojie L., Zhuangzhuang F. (2021). Measuring surface roughness of agricultural soils: Measurement error evaluation and random components separation. *Geoderma*, 404, 115393. https://doi.org/10.1016/j.geoderma.2021.115393
- 75. Xu C, Liu W, Li J, Wu J, Zhou Y Kader R. (2024). Dynamic change of soil aggregate stability and infiltration properties during crop growth under four

- tillage measures in Mollisols region of northeast China. *Frontiers in Earth Science 12*, 1357467. https://doi.org/10.3389/feart.2024.1357467
- 76. Yang Y., Meng Z., Li H., Gao Y., Li T., Qin L. (2025). Soil porosity as a key factor of soil aggregate stability: insights from restricted grazing. *Frontiers in Environmental Science* 12, 1535193. https://doi.org/10.3389/fenvs.2024.1535193
- 77. Zheng F., Liu X., Ding W., Song X., Li S., Wu X. (2023). Positive effects of crop rotation on soil aggregation and associated organic carbon are mainly controlled by climate and initial soil carbon content: A meta-analysis. Agriculture Ecosystems &

- Environment 355, 108600. https://doi.org/10.1016/j. agee.2023.108600
- 78. Zhou M., Liu C., Wang J., Meng Q., Yuan Y., Ma X., Liu X., Zhu Y., Ding G., Zhang J., Zeng X., Du W. (2020). Soil aggregates stability and storage of soil organic carbon respond to cropping systems on Black Soils of Northeast China. *Scientific Reports*, 10, 265. https://doi.org/10.1038/s41598-019-57193-1
- 79. Zhu G.Y., Deng L., Shangguan Z.P. (2018). Effects of soil aggregate stability on soil N following land use changes under erodible environment. *Agriculture, Ecosystems & Environment* 262, 18–28. https://doi.org/10.1016/j.agee.2018.04.012